

Additives, Blends, Block Copolymers, and Composites

Typically, commercial plastics are mixtures of one or more polymers and a variety of *additives* such as plasticizers, flame retardants, processing lubricants, stabilizers, and fillers. The exact formulation will depend upon the specific application or processing requirement. For example, poly(vinyl chloride) (PVC) is a thermally unstable polymer (see Section 6.1.1) having high modulus, or stiffness, typical of other glassy polymers at room temperature. In order to obtain a flexible-grade resin of PVC for use as packaging film or for wire insulation, the polymer must be blended with a plasticizer to reduce its T_g and with a small amount of an additive to improve its thermal stability at processing temperatures.

In many cases, certain properties of a polymer can be enhanced by blending it with another polymer. For example, the engineering thermoplastic, poly(2,6-dimethyl-1,4-phenylene oxide) (PPO), is a high- T_g polymer that is difficult to pro-

cess because of its susceptibility to thermal oxidation at high temperatures. Commercial resins of this polymer (Noryl) are blends of PPO and high-impact polystyrene (HIPS) and can also include different additives, such as lubricants, thermal stabilizers, flame retardants, or fillers. Since the T_g of PS (ca. 100°C) is lower than that of PPO (ca. 214°C), the overall T_g of the PPO/HIPS blend is lower than that of PPO alone and, therefore, the resin can be melt-processed at reduced temperatures where the oxidative instability of PPO is not a problem. The incorporation of HIPS also reduces the cost of this engineering resin and improves the impact strength of the blend.

Polymeric composites are physical mixtures of a polymer (the matrix) and a reinforcing filler (the dispersed phase) that serves to improve some mechanical property such as modulus or abrasion resistance. Fillers may be inorganic (e.g., calcium carbonate) or organic (graphite fiber or an aromatic polyamide such as Kevlar). Virtually any material can be used as the composite matrix, including ceramic, carbon, and polymeric materials. Typically, matrices for polymeric composites are thermosets such as epoxy or (unsaturated) polyester resin; however, some engineering thermoplastics with high T_g and good impact strength, such as thermoplastic polysulfones, have been used for composites. Principal applications for composites are in construction and transportation.

7.1 Additives

A variety of additives are widely used for thermoplastics, thermosets, and elastomers. The global market for plastics additives in 2011 was nearly \$40 billion and is expected to grow to about \$48 billion by 2016. Additives are sometimes grouped into four main functional categories—property modifiers, property extenders, stabilizers, and processing aids. Property modifiers represent the largest segment of the additives market. These include flame retardants, antioxidants, antimicrobials, plasticizers, blowing agents, and impact modifiers. Of these, plasticizers and flame retardants are the fastest-growing segment of this market. The plasticizer market is expected to grow by about 3.2% through 2016 and represents about 50% of the total additives market. In practice, additives are mixed with a polymer before processing by a variety of techniques, such as dry blending, extrusion, compounding, and other methods discussed later in Chapter 11.

7.1.1 Plasticizers

Plasticizers, particularly for PVC, constitute one of the largest segments of the additives market. The principal function of a plasticizer is to reduce the modulus of a polymer at the use temperature by lowering its T_g . The effect of a plasticizer on

modulus is illustrated by Figure 7-1. As shown, increasing the concentration of the plasticizer causes the transition from the high-modulus (glassy) plateau region to the low-modulus (rubbery) plateau region to occur at progressively lower temperatures. In addition, the transition of the plasticized polymer occurs over a wider range of temperatures than for the unplasticized polymer. Typically, plasticizers are low-molecular-weight organic compounds having a T_g in the vicinity of -50°C . In some cases, a miscible high-molecular-weight polymer having a low T_g (e.g., polycaprolactone or copolymers of ethylene and vinyl acetate) can be used as a plasticizer.

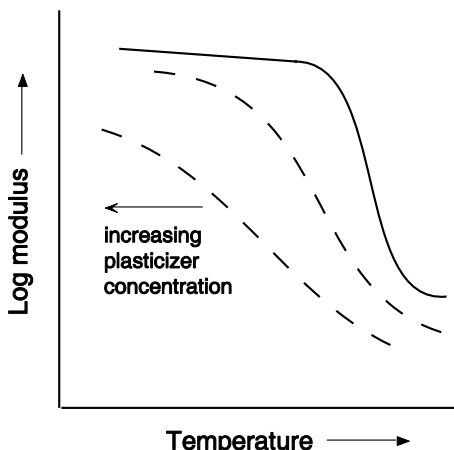


Figure 7-1 Effect of increasing plasticizer concentration on the modulus–temperature plot.

Requirements for an effective plasticizer include partial or complete miscibility with the host polymer and a low T_g . The T_g of the plasticized polymer depends upon the plasticizer concentration and the T_g of each component as estimated by a number of theoretical or empirical equations, such as the Kelley–Bueche equation [1] and others given in Section 4.3.4. Another commonly used relationship first proposed by Wood [2] to predict the T_g of random copolymers has been used to predict the T_g of plasticized polymers. The *Wood equation* has the form

$$T_g = \frac{T_{g,1} + (kT_{g,2} - T_{g,1})W_2}{1 - (1-k)W_2}. \quad (7.1)$$

In this equation, k is considered to be an adjustable parameter and W_i is the weight fraction of component i where component 1 is typically the diluent. A related equation is the *Gordon–Taylor equation* [3]

$$T_g = \frac{T_{g,1}W_1 + KT_{g,2}W_2}{W_1 + KW_2} \quad (7.2)$$

where K is also commonly taken to be a fitting parameter. The Gordon–Taylor equation has been shown to be successful for fitting the T_g of random copolymers [4] and is also widely used to model the composition dependence of polymer mixtures and blends.

A very convenient equation relating T_g to the composition of a polymer mixture from known parameters (composition and individual polymer T_g) was given in Chapter 4 (eq (4.34)) as

$$\ln\left(\frac{T_g}{T_{g,1}}\right) = \frac{W_2 \ln(T_{g,2}/T_{g,1})}{W_1(T_{g,2}/T_{g,1}) + W_2}. \quad (7.3)$$

Equation (7.3) has been shown to be useful for a wide variety of polymer mixtures, including polymer blends, for which the T_g s of both components are roughly comparable, and plasticized polymers such as PVC, for which the T_g s of the polymer and plasticizer are widely apart. Comparisons between experimental and predicted T_g values are shown for two polymer blends and plasticized PVC in Figure 7-2.

In the case of plasticization, the actual reduction in polymer T_g per unit weight of plasticizer is called the plasticizer *efficiency*. High efficiency indicates that the plasticizer causes the glassy-to-rubbery transition to occur over a very broad temperature range. The problem with high-efficiency plasticizers is that they can diffuse out of the polymer in time due to their low miscibility with the polymer. Plasticizers that are susceptible to migration are said to have low *permanence*. Loss of plasticizer will lead to a gradual increase in brittleness as the T_g (and, therefore, the modulus) of the plasticized polymer slowly increases to that of the unplasticized (i.e., glassy) polymer. An example of a high-permanence (i.e., low-efficiency) plasticizer for PVC is tris(2-ethylhexyl)trimellitate, sometimes called trioctyl trimellitate (TOTM) (see Table 7-1); T_g data for PVC plasticized with TOTM are plotted in Figure 7-1.

When T_g reduction is obtained by compounding a polymer with a low- T_g compound, the process is called *external plasticization*. In some cases, plasticizer function can be obtained by copolymerizing the polymer with the monomer of a low- T_g polymer, such as poly(vinyl acetate). This process is called *internal plasticization*.

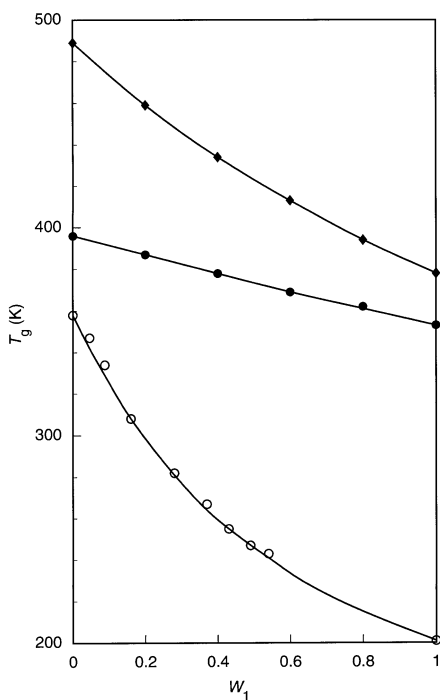
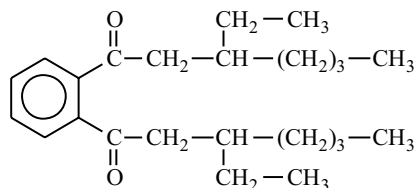


Figure 7-2 DSC-determined values of the glass-transition temperature (T_g) of two polymer blends and plasticized PVC as a function of the weight fraction (W_1) of the low- T_g component (component 1) [5]. Data include: (◆) poly(2,6-dimethyl-1,4-phenylene oxide)/polystyrene (1); (●) poly(vinyl chloride)/ α -methylstyrene-acrylonitrile-styrene (66/31/3) terpolymer (1); (○) poly(vinyl chloride)/tris-(2-ethylhexyl)trimellitate (TOTM) plasticizer (1). Solid curves represent T_g values predicted by eq. (7.3).

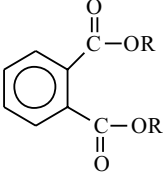
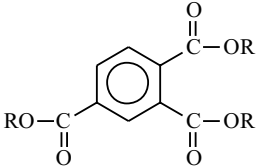
Typical external plasticizers for PVC include the esters of common organic acids such as dialkyl phthalates—examples include diisoctyl phthalate (DIOP) and di-2-ethylhexyl phthalate or dioctyl phthalate (DOP):



that has been a widely used high-efficiency plasticizer for PVC. Other PVC plasticizers include epoxides, such as epoxidized soybean oil; aliphatic diesters, such as

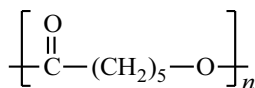
di-2-ethylhexyl adipate or dioctyl adipate (DOA); phosphates, such as tricresyl phosphate (TCP); and trialkyl trimellitates, such as tris(2-ethylhexyl trimellitate) or trioctyl trimellitate (TOTM). General structures for these classes of PVC plasticizers are shown in Table 7-1.

Table 7-1 Common Plasticizers for PVC

Plasticizer Classification	Chemical Structure	Examples ^a
Aliphatic diester	$\text{RO}-\overset{\text{O}}{\underset{\parallel}{\text{C}}}-\text{(CH}_2\text{)}_n-\overset{\text{O}}{\underset{\parallel}{\text{C}}}-\text{OR}$	DOA
Dialkyl phthalate		DOP, DIOP
Trialkyl phosphate	$\text{RO}-\overset{\text{O}}{\underset{\parallel}{\text{P}}}-\text{OR}'-\text{OR}''$	TCP
Trialkyl trimellitate		TOTM

^a Common names for plasticizers: DOP, dioctyl phthalate; DIOP, diisoctyl phthalate; DOA, dioctyl adipate; TCP, tricresyl phosphate; and TOTM, trioctyl trimellitate.

Examples of polymeric plasticizers include polycaprolactone (PCL):



with a T_g of -60°C and copolymers (and terpolymers) of ethylene with vinyl acetate, carbon monoxide, and sulfur dioxide. Polymeric plasticizers provide high permanence at the expense of low-temperature flexibility due to their higher T_g and low efficiency.

It has been observed that at low concentrations of plasticizer (e.g., 5% to 10%), modulus and tensile strength may sometimes be greater than that of the un-plasticized polymer, while impact strength and permeability to gases and liquids may be lower. This behavior is opposite to that usually associated with plasticization and is, therefore, known as *antiplasticization*. If the plasticizer concentration is

raised above the antiplasticization range, the modulus and tensile strength will begin to fall, while the impact strength and permeability will increase (i.e., plasticization begins).

7.1.2 Fillers and Reinforcements

Fillers for thermoplastics and thermosets may be inert materials that serve to reduce resin cost and (to a lesser extent) improve processability or dissipate heat in exothermic thermosetting reactions. Examples of such fillers include wood flour, clay, talc, fly ash, sand, mica, and glass beads. Mica can also be used to modify the polymer's electrical- and heat-insulating properties. Other particulate fillers may be used to reduce mold shrinkage or to minimize electrostatic charging. These include graphite, carbon black, aluminum flakes, and metal and metal-coated fibers. For example, high loading of carbon fibers can provide electromagnetic interference (EMI) shielding for computer applications.

Reinforcing fillers are used to improve some mechanical property or properties, such as modulus, tensile or tear strength, abrasion resistance, and fatigue strength. For example, particulate fillers such as carbon black or silica are widely used to improve the strength and abrasion resistance of commercial elastomers. Fibers in the form of continuous strands, woven fabrics, and chopped (or discontinuous) fibers are used to reinforce thermoplastics and thermosets.

The typical fiber content of a polymer composite may range from 20% to 80% of the total weight. The most common form of fiber fillers is E-glass, typically used to reinforce thermosets, such as (unsaturated) polyester and epoxy resins. E-glass is a boroaluminosilicate glass having low alkali-metal content and containing small percentages of calcia (CaO) and magnesia (MgO). For special applications, such as in the manufacture of aerospace materials, fibers of boron, Kevlar (an aromatic polyamide or aramid), and especially carbon or graphite are preferred. Carbon and graphite fibers are obtained by the pyrolysis of organic materials such as polyacrylonitrile (PAN), rayon, or pitch. The highest mechanical properties are obtained by orienting the fibers at temperatures as high as 3000°C (graphite fibers). At the expense of higher cost and increased brittleness, these specialized fibers provide higher composite strength and modulus than glass-reinforced composites. Recently, there has been interest in using ultrahigh-molecular-weight polyethylene (see Chapter 10), having strength equal to an aramid fiber, as fiber reinforcement for epoxy and other matrices.

In addition to improvement in mechanical properties, composites may also offer weight reduction and improved conductivity, such as are provided by carbon or graphite fibers. Properties of typical fiber materials are given in Table 7-2. For highly demanding applications, microfibers or whiskers (synthetically grown single crystals) of alumina or silicon carbide may be used. Whiskers can have tensile strengths as high as 27.6 GPa (4 million psi) and moduli as high as 690 GPa (100

million psi). Other composite fillers recently being considered include buckminsterfullerene, C₆₀, which has been found to increase both T_g and thermal stability. Carbon nanotubes have extremely high modulus (up to 1.8 GPa) and are less brittle than carbon fiber. These can be used to make conductive composites suitable for electrostatic painting.

Table 7-2 Properties of Fibers Used in Composite Applications

Fiber	Tensile Modulus GPa ^a	Tensile Strength GPa ^a	Density g cm ⁻³
Boron	386	3.4–3.7	2.38–2.66
E-glass	72.4	3.45	2.55
S-glass	85.5	4.83	2.49
Graphite			
High-modulus	483–517	1.86	1.97
High-strength	234–255	2.83	1.77
Kevlar-49	138	2.76	1.44
Steel	407	4.14	7.81

^a To convert GPa to psi, multiply by 145,000.

7.1.3 Other Important Additives

In addition to plasticizers and fillers, the other important additives found in commercial plastics include thermal stabilizers, antioxidants, and UV-stabilizers to protect sensitive polymers against degradation due to processing temperatures and environmental attack. Other additives are used to improve fire resistance, to meet certain processing requirements (lubricants, curing and blowing agents, and catalysts for polymers prepared by reaction injection molding), to improve impact strength, to protect against exposure to bacteria and fungi, and to impart color. The specific formulation of a plastics resin is finely tailored to the end use of the resin. Formulations of plastic resins are usually given on the basis of parts per 100 unit weight of resin (phr), where the resin refers to the base polymer in the composition. The methods of action and some examples of these important additives are described in the following sections.

An important example of the use of plastics additives is PVC resin designed for potable water pipe extrusion. As shown by the data given in Table 7-3, PVC resin designed for this particular application can include eight or more different additives. All the components are blended using a dry blending technique in a specially designed mixer and then continuously extruded through an annular die. For the representative formulation given in Table 7-3, an acrylic-type processing aid may be used to provide a smooth extrudate, while calcium stearate and paraffin wax are present as lubricants. Since it is necessary to provide rigidity for pipe applications,

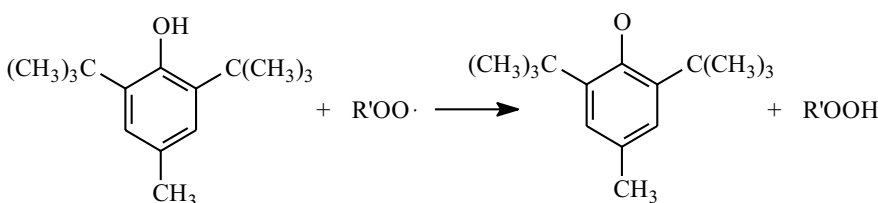
no plasticizers are used in this formulation. Ultrafine calcium carbonate is used as a reinforcing filler to provide high burst resistance. The choice of a thermal stabilizer depends upon consideration of toxicity levels since it is possible that plasticizer can diffuse out of the pipe into the water supply. For PVC pipe applications, alkyltin or antimony mercaptides are widely used stabilizers in the United States.

Table 7-3 Typical Formulation of a PVC Resin for Potable Water Pipe Extrusion

Component	Concentration (phr)
PVC (0.9 to 1.0 IV ^a)	100
Processing aids	1–5
Pigment	1–2
Calcium stearate	0.5–1.5
Paraffin wax	0.5–1
Alkyltin or antimony mercaptide	0.3–2.0
Impact modifier	0–10
Calcium carbonate	0–10

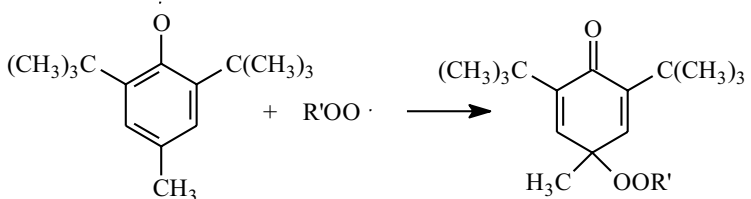
^a Inherent viscosity.

Stabilizers. Short-term stabilizers are those that are used to protect a polymer against the effects of temperature and oxygen during processing. These are typically low-molecular-weight compounds, such as hindered phenols and aromatic amines, which have high diffusivity in the polymer melt and serve as free-radical scavengers. Other antioxidants include those that serve to suppress homolytic breakdown such as organic phosphites. An example of an antioxidant that serves as a free-radical scavenger is 4-methyl-2,6-di-*tert*-butylphenol, which is used to inhibit the thermal oxidation of natural rubber. It functions by terminating free-radical sites formed as a result of thermal oxidation (see Section 6.1.1) by two routes: (1) abstraction of its hydroxyl hydrogen:

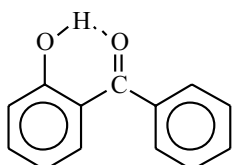


4-methyl-2,6-di-*tert*-butylphenol

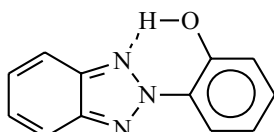
or (2) addition to the *para*-position of the aromatic ring:



Many polymers will absorb UV radiation in the wavelength from 290 to 400 nm. This absorbed energy can break bonds and initiate free-radical chain reactions that can lead to discoloration, embrittlement, and eventual degradation. UV stabilizers act to either absorb UV radiation or to deactivate free radicals and hydroperoxides as they are formed. As an example, carbon black, widely used in tire manufacture, provides good absorption in the UV range, as well as providing abrasion resistance and serving as a low-cost filler. Transparent thermoplastics like polycarbonate can be protected against yellowing and embrittlement from UV irradiation (photolysis) by incorporating compounds like benzophenone derivatives, such as *o*-hydroxybenzophenone:



These benzophenones have a high extinction coefficient in the UV range and are able to convert absorbed radiation to heat without chemical change. Benzotriazoles such as 2-(*o*-hydroxyphenyl)benzotriazole



are also widely used as UV absorbers.

Flame Retardants. When subjected to a sufficient heat flux for a sufficiently long time, all organic polymers will thermally degrade. Minimum radiant fluxes vary from about 16 to 34 kilowatts (kW) m^{-2} for polyurethane foam to 43 kW m^{-2} for polytetrafluoroethylene. In the absence of oxygen, thermal degradation is called *pyrolysis*. In the presence of oxygen, thermal degradation is called *oxidative pyrolysis* or *thermal-oxidative degradation*.

Flame retardants are added to alter the combustion process in some way. Strategies for effective flame retardants include the following:

- Inhibition of the vapor-phase combustion of the fuel gases
- Alteration of the thermal-degradation pathway by providing a low-energy process that promotes solid-state reactions leading to carbonization
- Formation of a protective coating to insulate against thermal energy

Classes of flame retardants include organochlorine compounds, organobromine compounds, organophosphorus, antimony oxides, boron compounds, and especially alumina trihydrate (ATH).

Biocides. In general, polyolefins and vinyl polymers are particularly resistant to bacterial attack (see Section 6.2.3) while natural rubber, cellulose and cellulose derivatives, and some polyesters are susceptible to microbial attack. A *biocide* is a chemical that controls or destroys bacterial growth. Alternative terminology includes bactericides, bacteristats, mildecides, fungicides, fungistats, germicides, and algicides. Important applications for biocides include latex paints and textiles. The ideal biocide is one that is toxic to the targeted microorganism but otherwise safe to humans and other animal life. For food packaging applications, biocides must be approved by the Food and Drug Administration in the United States. All biocides must be registered by the Environmental Protection Agency for use in the United States. Examples of industrial biocides include tributyltin oxide used in latex paints, textiles, and plastics and 10,10'-oxybisphenoxyarsine (OBPA) used in vinyl and urethane-polyolefin formulations.

Processing Additives. Lubricants are added to improve flow during processing by reducing melt viscosity (internal lubricants) or by reducing adhesion between metallic surfaces of the processing equipment and the polymer melt (external lubricants). Principal categories of lubricants include amides, esters, metallic stearates, waxes, and acids. The major market for processing lubricants is PVC, for which stearates are often used. Other lubricants include mineral oil and low-molecular-weight polyolefins. Organofunctional silicone fluids may be used as internal mold-release agents for reaction injection molding (RIM) of polyurethane (see Section 11.1.2).

Curing Agents. The term *curing* typically refers to the process of applying heat (and pressure) to change the properties of rubber or thermosetting resins. In the curing process, various additives (i.e., curing agents), including a number of sulfur-containing compounds, are used to promote the crosslinking of rubber (i.e., vulcanization) or the formation of a thermoset network (e.g., amines in the cure of epoxies). The process of network formation is discussed in detail in Chapter 9.

Colorants. Plastics can be colored by adding soluble dyes and inorganic and organic pigments that are dispersed in the plastic during processing. In the coloring of thermosets, dye dissolution or pigment dispersion must be completed before the

thermoset is fully formed. Classes of dyes that are used for plastics include azo compounds, anthraquinones, xanthenes, and azines. Among the most important inorganic pigments are iron oxides, cadmium, chrome yellow, and especially titanium dioxide (white).

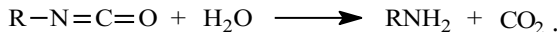
Heat Distortion and Impact Modifiers. Blends of one polymer with another having greater or lower T_g can be used to modify the T_g or heat-distortion temperature (HDT) of another polymer, as described in Section 7.2.2. Impact modifiers normally include high-impact polystyrene (HIPS), chlorinated polyethylene (CPE), and a variety of copolymers and terpolymers, such as SAN (styrene–acrylonitrile), ABS (acrylonitrile–butadiene–styrene), EVA (ethylene–vinyl acetate), MBS (methyl methacrylate–butadiene–styrene), and MABS (methyl methacrylate–acrylonitrile–butadiene–styrene). The mechanism of toughening is discussed in Section 7.2.2.

Antistatic Agents. Since most polymers are poor electrical conductors (see Section 12.3.1), static electrical charges can form on the surface of plastics. Such static charge buildup can present problems such as dust collection and sparking. Fortunately, hygroscopic additives called *antistats* are effective for dissipating static electrical charges. Antistats belong to either of two categories—external or internal. External, or topical, antistats are applied by spraying, wiping, or dipping the plastic surface, while internal antistats are compounded with the plastic during processing. In the case of internal antistats, the additive diffuses to the surface of the plastic where the hygroscopic additive absorbs moisture and, thereby, provides a conductive layer of water. Examples of antistatic agents include phosphate and fatty acid esters, polyhydric alcohol derivatives, sulfated waxes, ethoxylated and propoxylated aliphatics and aromatics, and especially quaternary ammonium compounds and amines.

Blowing Agents. Many plastics, such as polystyrene (expanded polystyrene) and polyurethanes, are foamed to provide insulating properties (rigid foam) or flexible products (flexible foam) for seat cushions and other applications. Gas production is achieved by adding a gas-producing compound called a *blowing agent* (or foaming agent). *Physical* blowing agents include volatile liquids such as short-chain hydrocarbons (e.g., pentanes, hexanes, and heptanes) and fluorocarbons (e.g., trichloromethane, tetrachloromethane, and trichlorofluoromethane) and gases such as nitrogen, carbon dioxide, and air that are added during processing. Volatilization results in the formation of a cellular structure through a phase change as the gas dissolved in the polymer at high pressure at processing conditions desorbs during depressurization. *Chemical* blowing agents (CBA) such as hydrazine derivatives are solid additives that generate gases when decomposed at processing temperatures. Unsaturated polyester is foamed by the use of a CBA. In some cases, gas production may occur by chemical reaction of the CBA with another component of the polymer system. Concern over emission of volatile organic compounds (VOCs), especially

chlorohydrocarbons, during processing has encouraged the development of safer alternatives to many of the physical blowing agents now used.

In the case of polyurethanes, flexible foams are produced by the production of carbon dioxide from the reaction of an isocyanate and water:



When the isocyanate is in excess, the resulting amine can react with another molecule of isocyanate to form a urea as shown:



Rigid foams are produced by use of a physical blowing agent, such as trichlorofluoromethane (refrigerant 11) or pentane. An important example of a rigid foam is expandable polystyrene (EPS) used for disposable drinking cups, cushioned packaging, and thermal insulation. The physical blowing agent used for EPS is typically pentane.

Compatibilizers. As discussed in the following sections, many polymers are immiscible and, therefore, phase-separate during processing. The mechanical properties of these immiscible blends are often poor due to inadequate interfacial strength between the dispersed phase and matrix. A variety of additives can be used to promote miscibility by reducing interfacial tension. Reactive compatibilizers chemically react with blend components and are, therefore, effective for many blend compositions. Nonreactive compatibilizers are typically block or graft copolymers of the blend homopolymers and are more specific in their action.

7.2 Polymer Blends and Interpenetrating Networks

7.2.1 Polymer Blends

The blending of two or more polymers has become an increasingly important technique for improving the cost/performance ratio of commercial plastics. For example, blending may be used to reduce the cost of an expensive engineering thermoplastic, to improve the processability of a high-temperature or heat-sensitive thermoplastic, or to improve impact resistance. Commercial blends may be homogeneous, phase-separated, or a bit of both.

Thermodynamics. Whether a particular polymer blend will be homogeneous or phase-separated will depend upon many factors, such as the kinetics of the mixing process, the processing temperature, and the presence of solvent or other addi-

tives; however, the primary consideration for determining miscibility of two polymers is a thermodynamic issue that is governed by the same (Gibbs) free-energy considerations that were discussed in Chapter 3 for polymer–solvent mixtures. The relationship between the change in Gibbs free energy due to mixing (ΔG_m) and the enthalpy (ΔH_m) and entropy (ΔS_m) of mixing for a reversible system was given as

$$\Delta S_m = \Delta H_m - T\Delta G_m. \quad (7.4)$$

If ΔG_m is positive over the entire composition range at a given temperature, the two polymers in the blend will separate into phases at equilibrium. For complete miscibility, two conditions are necessary: ΔG_m must be negative and the second derivative of ΔG_m with respect to the volume fraction of component 2 (ϕ_2) must be greater than zero

$$\left(\frac{\partial^2 \Delta G_m}{\partial \phi_2^2} \right)_{T,p} > 0 \quad (7.5)$$

over the entire composition range.

If $\Delta G_m < 0$, but eq. (7.5) is not satisfied (i.e., the appearance of local minima in the free-energy curve as shown in Figure 3-9), the blend will separate at equilibrium into two mixed-composition phases. This means that each phase (i.e., the dispersed and continuous phases) will contain some of each polymer. At a given temperature, equilibrium concentrations are given as a pair of isothermal points along the binodal ($\mu_i^A = \mu_i^B$), which is illustrated for a representative phase diagram in Figure 7-3.

In general, polymer blends can exhibit a wide range of phase behavior, including upper and lower critical solution temperatures (see Section 3.2.4), as illustrated by the liquid–liquid phase diagram given in Figure 7-3. At temperature T_1 , which is below the upper critical solution temperature (UCST) for phase separation located at T_2 , the equilibrium mixture will separate into two phases whose compositions lie on opposite sides of the *binodal* at T_1 . The binodal separates the stable (single phase) from the metastable state, while the *spinodal* marks the transition from the unstable to metastable region. At T_3 , which is above the UCST but below the lower critical solution temperature (LCST) located at T_4 , the blend is miscible at all compositions. Above the LCST (e.g., at T_5), two phases again coexist with compositions given by the upper binodal.

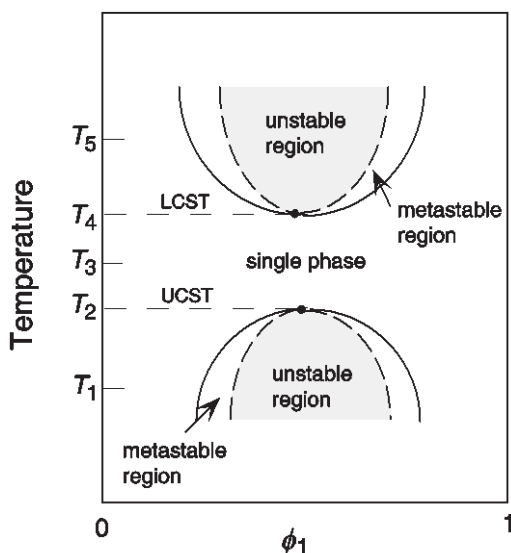


Figure 7-3 Idealized phase diagram for a polymer blend. The solid curve indicates a binodal, while the broken curve represents a spinodal separating the unstable and metastable regions. The upper critical (UCST) and lower critical solution (LCST) temperatures are located at T_2 and T_4 , respectively.

For polymer blends in the solid state, recent studies have shown that LCST behavior is quite common and needs to be considered during melt processing when elevated temperatures can cause phase separation and result in deleterious changes in the properties of the blend. An example of LCST phase behavior is a blend of polystyrene with the polycarbonate of tetramethylbisphenol-A [6]. In this case, a phase diagram was obtained by determining the temperature at which a particular blend composition first scatters light due to the incipient phase separation. Data obtained over the entire composition range are used to form a *cloud-point curve*. As shown by the data plotted in Figure 7-4, the LCST (assigned to the temperature at the minimum of the cloud-point curve) occurs near 240°C for this blend. This means that if the blend is melt-processed above 240°C, phase separation will occur. If the blend is heated above the LCST and rapidly cooled, the two-phase morphology will be retained in the solid state. As will be discussed shortly, thermal and mechanical properties will be very different depending on whether the blend forms a homogeneous mixture or a two-phase structure.

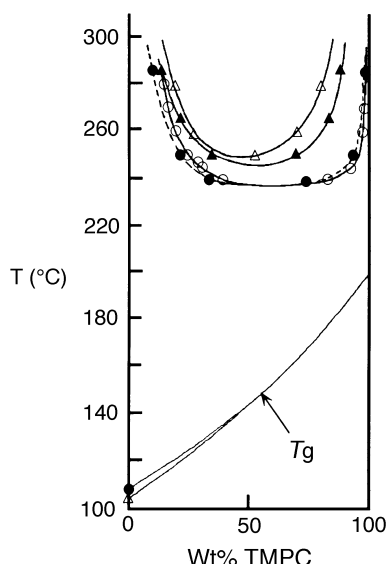


Figure 7-4 Phase behavior of TMPC/PS blends. Bottom curves show the dependence of T_g on the wt% of TMPC below the LCST. The top curves are cloud-point curves illustrating LCST behavior. The LCST shifts upward in temperature with decreasing PS molecular weight and the cloud-point curves are skewed toward the low-molecular-weight component, TMPC ($M_w = 41,000$). Molecular weights (M_w) of PS: (Δ), 42,000; (\blacktriangle), 59,000; (\circ), 180,000; and (\bullet), 320,000. Adapted with permission from K. H. Illers, W. Heckmann, and J. Hambrecht, *Untersuchung des Mischungsgleichgewichts binärer Polymermischungen. I. Mischungen aus Polystyrol und Tetramethyl-bisphenol A-Polycarbonat*. Colloid and Polymer Science, 1984. **262**: p. 557–565. Copyright 1984 Springer-Verlag.

Compared to LCST phase behavior, UCST behavior is much more difficult to observe since a UCST may fall below the blend T_g , at which temperature all long-range (cooperative) segmental motions cease. Such chain mobility is required to achieve phase separation. For this reason, UCST behavior may be observed only in a solution of the blend in a low-molecular-weight solvent or under other special circumstances.

The bulk of experimental evidence indicates that most polymer pairs are immiscible. Immiscibility is a consequence of the very small combinatorial entropy change that results when two high-molecular-weight polymers are mixed. Scott [7] has extended the Flory–Huggins (F–H) lattice model (Section 3.2.1) to obtain an expression for ΔS_m for a polymer blend as

$$\Delta S_m = \left(\frac{RV}{V_r} \right) \left[\left(\frac{\phi_1}{x_1} \right) \ln \phi_1 + \left(\frac{\phi_2}{x_2} \right) \ln \phi_2 \right] \quad (7.6)$$

where R is the ideal gas constant, V is the volume of the blend, V_r is a reference volume (often taken as the molar volume of the smallest polymer repeating unit), ϕ_i is the volume fraction of polymer 1 or 2, and x_i is the degree of polymerization of polymer 1 or 2 relative to the reference volume. The corresponding equation for the Gibbs free energy of mixing is then

$$\Delta G_m = \left(\frac{RTV}{V_r} \right) \left[\left(\frac{\phi_1}{x_1} \right) \ln \phi_1 + \left(\frac{\phi_2}{x_2} \right) \ln \phi_2 + \chi_{12} \phi_1 \phi_2 \right] \quad (7.7)$$

where χ_{12} is the (Flory) interaction parameter of the blend of polymers 1 and 2.

Since the degree of polymerization (x_1 and x_2 appearing in the denominators on the RHS of eq. (7.6)) of high-molecular-weight polymers is large, ΔS_m is small. In order for ΔG_m (eq. (7.4)) to be negative as a necessary condition of miscibility, the enthalpic contribution to mixing, ΔH_m , must be either negative or zero, or have a small positive value. This implies that blend miscibility requires favorable interactions between the two blend polymers. Examples of favorable interactions include dispersive and dipole–dipole interactions, hydrogen bonding, or charge-transfer complexation.

As discussed in Chapter 3, the Flory–Huggins theory, although providing a useful basis for discussion, fails to correctly predict all aspects of polymer-blend behavior. For example, the F–H theory does not predict LCST behavior, which has been shown to occur. Good qualitative predictions of polymer phase behavior are, however, provided through the Flory equation of state (EOS) and other EOS models. For example, the effect of polymer molecular weight on the phase behavior of a binary polymer blend is qualitatively well represented using a modified form of the Flory EOS theory given by McMaster [8]. As shown in Figure 7-5, the LCST moves down in temperature as the molecular weight of either polymer in the blend decreases. This means that the region of miscibility increases with decreasing molecular weight, as may be expected from the favorable effect of decreasing molecular weight on increasing the combinatory entropy of the blend. Also evident is the skewness of the binodal and spinodal curves when chain lengths of the molecular weight of the two polymers considerably differ. Specifically, the critical composition moves to the left as the ratio of chain lengths r_1/r_2 decreases. Figure 7-6 shows the effect of changes in the value of the interaction parameter on the phase diagram. As shown, the LCST moves to higher temperatures and the miscibility window (the area outside the binodal) widens as the interaction energy decreases.

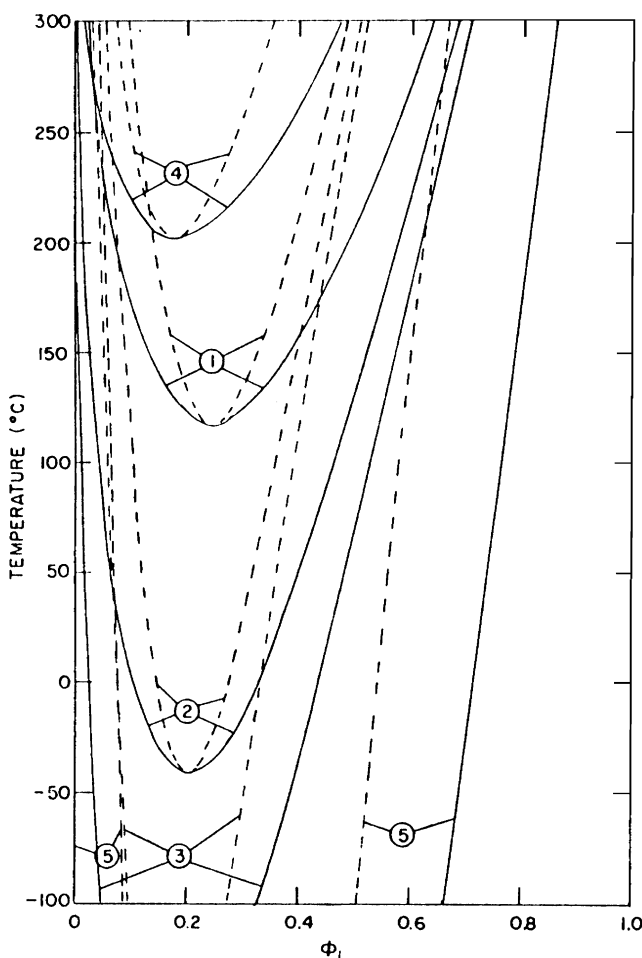


Figure 7-5 Effect of molecular weight of polymer 1 (curve 1, 30,000 molecular weight; curve 2, 50,000 molecular weight; and curve 3, 80,000 molecular weight) and polymer 2 (curve 4, 3000 molecular weight; curve 5, 6000 molecular weight) on the binodal (solid line) and spinodal (broken line) predicted by a modified version of the Flory EOS theory. Adapted with permission from L. P. McMaster, *Aspects of Polymer-Polymer Thermodynamics*. Macromolecules, 1973. 6: p. 760–773. Copyright 1973, American Chemical Society.

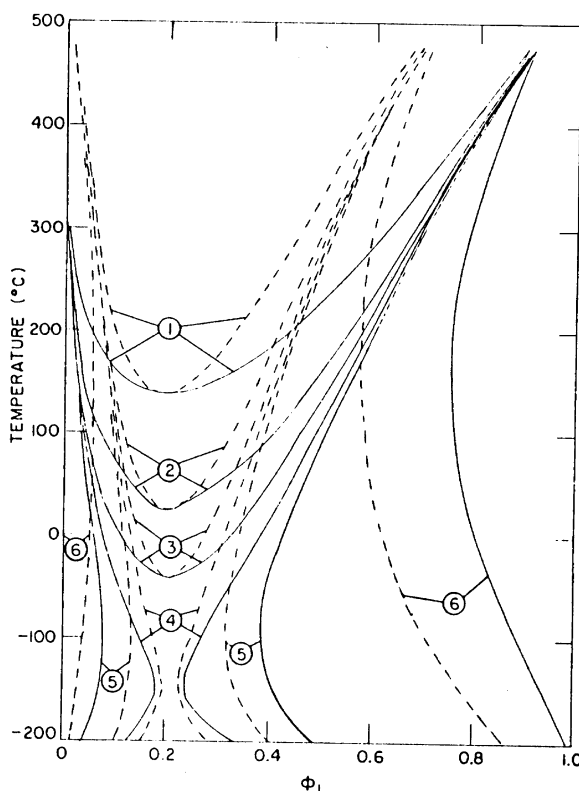


Figure 7-6 Effect of the value of the interaction energy on the binodal (solid line) and spinodal (broken line) predicted by a modified version of the Flory EOS theory. Values of X_{12} (cal cm^{-3}): curve 1, -0.050; curve 2, -0.100; curve 3, 0; curve 4, 0.005; curve 5, 0.010; and curve 6, 0.100. Adapted with permission from L. P. McMaster, *Aspects of Polymer-Polymer Thermodynamics*. Macromolecules, 1973. 6: p. 760–773. Copyright 1973, American Chemical Society.

Recently, there has been interest in blends containing three-component polymers. The phase behavior of these ternary blends is difficult to determine experimentally as well as difficult to theoretically predict and to visualize. One way of representing their phase behavior is through the use of the triangular diagrams familiar to chemical engineers who have studied liquid–liquid equilibrium. The experimentally determined phase diagram [9] for ternary blends of PMMA, poly(ethyl methacrylate) (PEMA), and poly(styrene-*co*-acrylonitrile) (SAN) is shown in Figure 7-7. In this example, SAN (30 wt% acrylonitrile) is compatible (miscible) with PMMA and PEMA; however, PMMA and PEMA, themselves, are immiscible. In other words, two of the three polymer pairs are immiscible. As illustrated, there is a

moderately wide range of compositions (represented by the open circles lying outside the phase envelope) for which the three polymers can exist as homogeneous mixtures even though one polymer pair (PMMA/PEMA) is immiscible. In this study, evidence for phase homogeneity was deduced from detection of a single T_g (DSC measurements) for the blend.

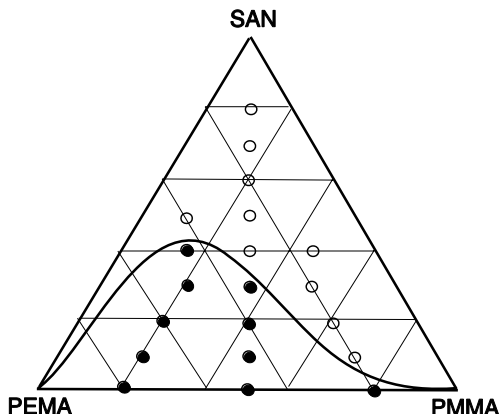


Figure 7-7 Triangular phase diagram for ternary blends of poly(methyl methacrylate) (PMMA), poly(ethyl methacrylate) (PEMA), and poly(styrene-co-acrylonitrile) (SAN). Filled circles (●) represent blend compositions that are phase-separated as indicated by the detection of multiple T_g s. Open circles (○) represent homogeneous compositions. Adapted from S. H. Goh and K. S. Siow, *Calorimetric Study of the Miscibility of Poly(styrene-co-acrylonitrile)/Poly(methyl methacrylate)/Poly(ethyl methacrylate) Ternary Blends*, *Thermochimica Acta*, 1985. **105**: p. 191–195, Copyright 1986, with permission from Elsevier Science.

Commercial Polymer Blends. Well-documented examples of miscible polymer blends are given in Table 7-4. Of these, the blends of poly(2,6-dimethyl-1,4-phenylene oxide)/PS and PVC/nitrile rubber (a copolymer of butadiene and acrylonitrile) are important commercially. Blends of poly(methyl vinyl ether)/PS and tetramethylbisphenol-A polycarbonate/PS, as mentioned earlier, have been reported to exhibit LCST at melt temperatures and have been widely used to study polymer-blend behavior. All these blends consist of only amorphous polymers, with the exception of PVC, which has a small degree of crystallinity (see Section 9.1.2).

In the case of poly(vinylidene fluoride) (PVDF) blends, PVDF can thermally crystallize depending upon blend composition and crystallization temperature. The second (amorphous) polymer in the blend (i.e., PEEMA or PMMA) serves as a diluent, which lowers the crystalline-melting temperature, T_m , of the blend. From this information, the Flory interaction parameter can be obtained as discussed in Chapter 4 (eq. (4.4)). A plot of the T_g of the miscible [10] is shown in Figure 7-8.

Table 7-4 Examples of Miscible Polymer Blends

Polymer 1	Polymer 2
Polystyrene	Poly(2,6-dimethyl-1,4-phenylene oxide) Poly(methyl vinyl ether) Tetramethylbisphenol-A polycarbonate
Poly(vinyl chloride)	Polycaprolactone Nitrile rubber ^a
Poly(vinylidene fluoride)	Poly(ethyl methacrylate) Poly(methyl methacrylate)

^a For limited acrylonitrile content of the copolymer.

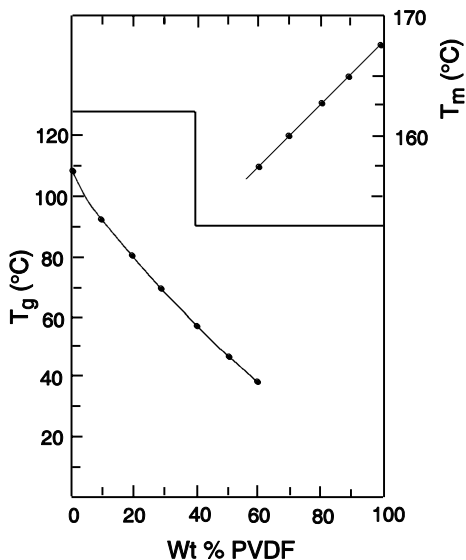


Figure 7-8 Experimental (DTA) values of T_g and T_m as a function of wt% of poly(vinylidene fluoride) (PVDF) in PVDF/PMMA blends. Adapted with permission from D. R. Paul and J. O. Altamirano, in *Copolymers, Polyblends, and Composites*, N. A. J. Platzer, ed., Advances in Chemistry Series No. 142, 1975, Washington, DC: American Chemical Society p. 371–385. Copyright 1975, American Chemical Society.

Properties of Blends. Properties of miscible polymer blends may be intermediate between those of the individual components (i.e., additive behavior), as is typically the case for T_g (see Figure 7-2). In other cases, blend properties may exhibit either positive or negative deviation from additivity, as illustrated by Figure 7-9. For example, both modulus and tensile strength of miscible polymer blends exhibit

a small maximum at some intermediate blend composition, while impact strength and permeability (see Chapter 12) will normally go through a broad minimum. This latter behavior has been attributed to a loss in free volume corresponding to a negative volume change of mixing (ΔV_m) due to favorable interactions between blend polymers.

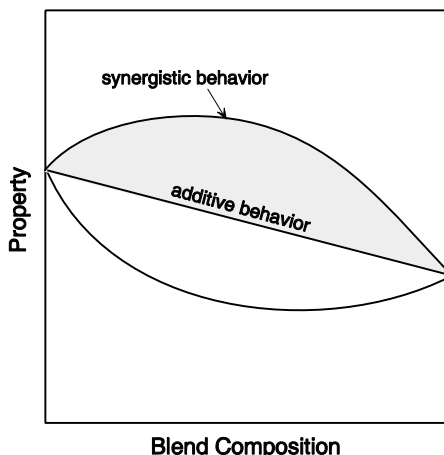


Figure 7-9 Illustration of three types of behavior for the dependence of miscible blend properties on composition.

7.2.2 Toughened Plastics and Phase-Separated Blends

The impact strength of brittle plastics such as PS can be significantly improved by incorporating a rubbery phase (e.g., polybutadiene) in the form of small (< 0.01- μm -diameter) dispersed particles. Provided that adhesion between the dispersed phase and matrix polymer is good, the rubber particles can provide an energy-absorbing capability through a change in the mechanical-deformation process either through promotion of extensive shear yielding or craze formation (see Section 4.4.1) or through a combination of both. In the case of high-impact polystyrene (HIPS), interfacial adhesion is promoted by graft polymerization of butadiene with the polystyrene matrix.

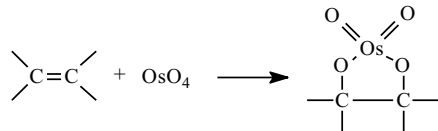
Figure 7-10 shows the complex morphology and extensive craze structure of a typical sample of HIPS that has undergone tensile deformation [11]. The phase structure is clearly seen in Figure 7-10A, which is a transmission electron micrograph of a sample that had been deformed, microtomed, and stained with osmium

tetroxide.* The light-colored areas contain the unstained polystyrene component of HIPS while the stained polybutadiene (PBD) regions appear as the darkened areas. It is noted that the dispersed PBD particles, which range in size from approximately 0.1 to 1.0 μm in diameter, contain significant amounts of occluded PS. These particles also appear to have become spheroidal as a result of the deformation process. The thin dark lines are the crazes (oriented perpendicular to the tensile direction) that have survived the microtoming and staining procedures. As a result of the removal of strain prior to sample preparation, the crazes have had an opportunity to relax or "heal" and therefore appear as thin, rather featureless structures. Extensive crazing is more clearly seen in Figure 7-10B, which shows a micrograph of the same sample that was obtained by deforming an unstained thin (0.1 μm) section that had been bonded to a copper cartridge inside the electron micrograph. In this case, the dispersed phase is less distinct due to the absence of staining; however, the craze microstructure is fully developed with the crazes interconnecting the dispersed PBD particles. As before, the crazes are oriented perpendicular to the tensile direction but the fibrils within the unrelaxed crazes are now clearly seen to be aligned in the tensile direction. This type of craze proliferation and bifurcation provides a means of energy dissipation (i.e., toughening) in the otherwise brittle PS matrix.

A higher-heat-distortion version of HIPS is ABS, which is an impact-modified styrene–acrylonitrile copolymer. Both HIPS and ABS are blended with other polymers to improve impact strength, as in the case of some commercial resins of polycarbonate (ABS-modified), PVC (ABS-modified), and poly(2,6-dimethyl-1,4-phenylene oxide) (HIPS-modified). Other polymeric impact modifiers include chlorinated polyethylene (CPE) and a variety of important copolymers including ethylene–vinyl acetate (EVA), methyl methacrylate–butadiene–styrene (MBS), and methyl methacrylate–acrylonitrile–butadiene–styrene (MABS).

Heat-distortion temperature (HDT) of a given polymer can sometimes be improved by blending with a high-HDT polymer. An example is the blend of PVC ($T_g \approx 85^\circ\text{C}$) and copolymers of styrene and maleic anhydride ($T_g \approx 116\text{--}123^\circ\text{C}$). Additional applications for heterogeneous (i.e., phase-separated) polymer blends include

* Osmium tetroxide (OsO_4) is a stain widely used to provide electron contrast for transmission electron microscopy of unsaturated polymers. This stain reacts with carbon double bonds as shown below and, in addition to providing increased electron density, serves to harden the rubbery component (e.g., polybutadiene in HIPS and ABS) and, therefore, facilitates sectioning by use of a cryogenic microtome.



coextruded textile polymers for the purpose of modifying some fiber property such as dyeability, self-crimping behavior, or antistatic character. In all these instances, acceptable mechanical properties of the blend require good interfacial adhesion between the continuous and dispersed phases. In the extreme case of macrophase-separated blends, mechanical properties as well as film clarity (i.e., transparency) may be unacceptable. In such cases, *compatibilizing agents* such as block copolymers containing one or two of the blend polymers may be useful to improve interfacial coupling.

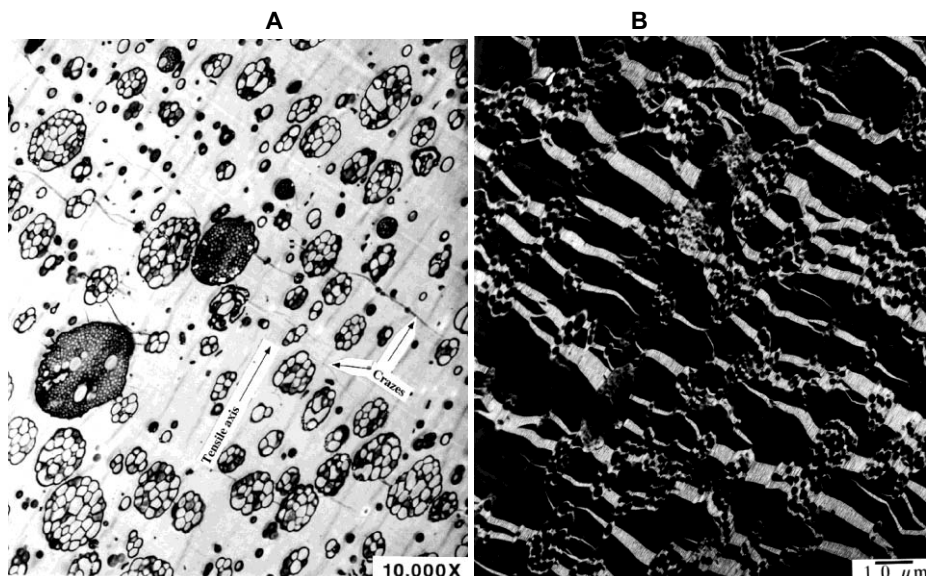


Figure 7-10 Transmission electron micrographs of high-impact polystyrene (HIPS). **A.** Stained microtomed section. **B.** In situ crazing using specimen deformation cartridge. Courtesy of R. C. Cieslinski, The Dow Chemical Company.

7.2.3 Interpenetrating Networks

Interpenetrating polymer networks or IPNs are combinations of two or more polymers in network form. At least one of the polymers is synthesized and/or cross-linked in the presence of the other. As such, IPNs share some of the advantages of both polymer blends and network polymers. If the two polymers in an IPN are thermodynamically immiscible, phase separation will occur as the monomer or monomers polymerize; however, the size of the dispersed phase will be smaller (10 to 100 nm) than would be the case for a physically mixed blend or for a block copolymer or graft of the two components. The controlled phase separation is due to

crosslinking restricting chain motion of the IPN. A wide range of morphologies is possible, depending upon the volume fraction of components, the viscosity of the phases, and the relative rates of crosslinking and phase separation.

Polymers that can be used in the preparation of IPNs include polyurethanes, polystyrene, poly(ethyl acrylate), and poly(methyl methacrylate). One of the earliest commercialized IPNs, used in many automotive applications, consists of polypropylene and ethylene-propylene-diene terpolymer (EPDM). If the ethylene segments of EPDM are sufficiently long to crystallize, the components are held together by crystalline domains of both polymers without the need of crosslinking (i.e., a thermoplastic IPN).

There are several ways by which IPNs can be prepared. For example, a *sequential IPN* is formed by first crosslinking one polymer. The crosslinked network is then swollen with a mixture of a monomer of the second polymer and a suitable crosslinking agent. The swollen film is then heated to initiate the polymerization and to crosslink the second (interpenetrating) network. An example of an IPN of poly(ethyl acrylate) (PEA) and polystyrene prepared in this way is illustrated in Figure 7-11.

If no crosslinking agent is used for the second polymer in the formation of a sequential IPN, only a single network of the initial polymer will result. In this case, the interpenetrating network is called a *semi-IPN*. *Gradient IPNs* are prepared by polymerizing the second monomer before equilibrium sorption occurs. *Simultaneous interpenetrating networks* (SINs) are formed when both polymers are synthesized and crosslinked simultaneously. Normally, SINs utilize polymers with different polymerization mechanisms (i.e., step and chain growth) to eliminate the possibility of copolymerization of the two monomers. Potential applications of IPNs include toughened plastics, ion-exchange resins, pressure-sensitive adhesives, soft contact lenses, controlled-release of drugs, and the preparation of novel membrane systems and sound- and vibration-damping material.

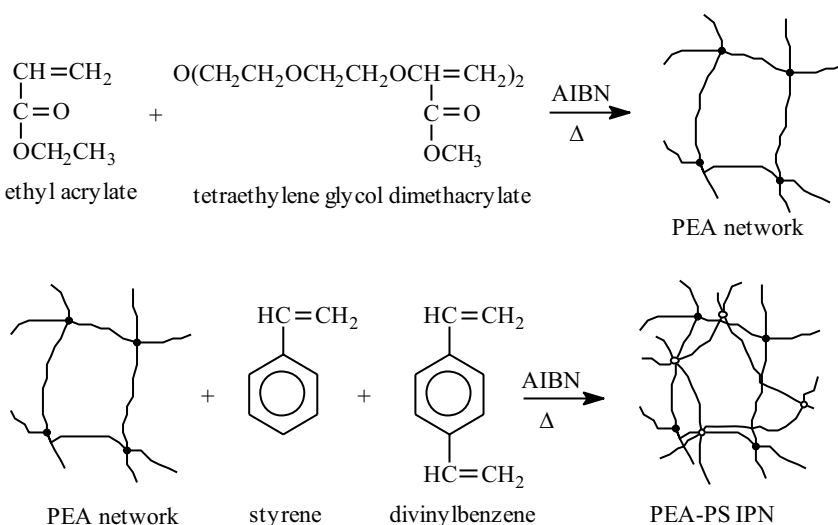


Figure 7-11 Preparation of a sequential interpenetrating network (IPN) by first polymerizing ethyl acrylate with a difunctional monomer, tetraethylene glycol dimethacrylate. The resulting PEA network is then swollen with styrene and divinylbenzene, which are subsequently polymerized to form an interpenetrating polystyrene network. The resulting IPN may be termed *cross-poly(ethyl acrylate)-inter-cross-polystyrene*, where the connectives *cross* and *inter* indicate crosslinked and interpenetrating, respectively. Adapted from L. W. Barrett and L. H. Sperling, *Today's Interpenetrating Polymer Networks*, Trends in Polymer Science, 1993, 1: p 45–49. Copyright 1993, with permission from Elsevier Science.

7.3 Block Copolymers

Polymerization of block and triblock copolymers by a number of different polymerization schemes including anionic, RAFT, group transfer, and click chemistry was covered in Chapter 2 (i.e., Sections 2.2, 2.4, and 2.5). Triblock copolymers such as polystyrene-*b*-polybutadiene-*b*-polystyrene (SBS) have applications as thermoplastic elastomers and are covered in Section 9.2.3. Amphiphilic triblock copolymers containing end blocks of hydrophilic polymers such as poly(ethylene oxide) or poly(2-alkyl-oxazolines) with a hydrophobic middle block such as polydimethylsiloxane or poly(ethyl ethylene) are being used to prepare biomimetic bilayers in which a variety of proteins are able to self-assemble into functional membrane

structures [12]. For all these reasons, how AB, ABA, and ABC* block copolymers self-organize into specific morphological structures in solution or in the melt and how different morphologies affect properties and function has significant importance. As discussed in Sections 2.2.1 and 2.2.2, physical blends of immiscible polymers will phase-separate at equilibrium. In the case of di- or triblock copolymers, the individual polymer blocks are prevented from complete macroscopic separation by their physical attachment to each other. The consequence is that the dimensions of the resulting structures are small (in the order of the radius of gyration). Energetically, phase separation is controlled by a competition between the drive to minimize the interfacial energy between immiscible polymers and the maximization of segmental entropy that decreases upon chain extension.

Self-assembly. In the case of diblock copolymers, such as polystyrene-*b*-polyisoprene and polystyrene-*b*-polybutadiene, the phase structure is controlled by the overall degree of polymerization, N , the overall volume fraction, f , and the Flory–Huggins interaction parameter (see Section (3.2.1)) between blocks A and B (χ_{AB}). The transition from a homogeneous melt to a micro-phase structure is termed the *order-disorder transition* and occurs at a critical value of the product χN . For a symmetric diblock copolymer where $f_A = f_B = 0.5$, this critical value is 10.5. Since χ is inversely proportional to temperature (see eq. (3.31), Section 3.2.1), a reduction in temperature will increase χ (and χN) and will eventually result in local ordering as shown by experimental data in Figure 7-12. Calculation of the phase diagram using self-consistent mean-field theory [13] shows good agreement with experimental results [14].

Due to their small dimensions, techniques such as TEM, SAXS, and small-angle neutron scattering (SANS) have been widely used for characterizing the morphology of block copolymers. TEM micrographs showing the morphology of two samples of polyisoprene-*b*-polystyrene (PI-PS) with different PI content and slightly different molecular weights are shown in Figure 7-13. The copolymer with the lower PI content (Figure 7-13a) exhibits lamellar microstructure while the copolymer with the higher PI content shows hexagonally packed cylinders (Figure 7-13b) in agreement with the predictions of self-consistent mean-field theory as mentioned in the previous paragraph.

* ABC block copolymers have three distinct polymer blocks—A, B, and C.

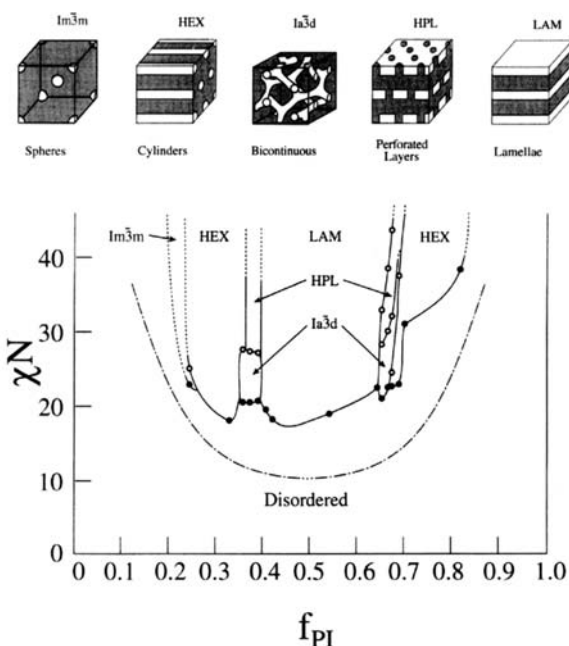


Figure 7-12 Experimental phase diagram for polyisoprene-*b*-polystyrene identifying regions of different morphologies such as body-centered close-packed spheres (Im^3m), hexagonal close-packed cylinders (HEX), and bicontinuous gyroid (Ia^3d) and lamellar structures (LAM). Reproduced with permission from A. K. Khandpur, et al., *Polyisoprene-Polystyrene Di-block Copolymer Phase Diagram near the Order-Disorder Transition*. *Macromolecules*, 1995. **28**: p. 8796–8806. Copyright 1995, American Chemical Society.

In the case of diblock containing one insoluble and one soluble block in water or other solvent, phase separation can occur in a variety of structures illustrated in Figure 7-14 [15]. The resulting geometry depends upon the concentration and the volume ratio between soluble and insoluble blocks (ISR). At a critical aggregation concentration (CAC), block copolymers begin to self-assemble into dispersed isotropic phases. The CAC decreases with increasing molecular weight and ISR composition. Assembled structures as diverse as polymer micelles and bilayer membranes can form (Figure 7-14). A key parameter is the packing parameter defined as

$$p = \frac{v}{a_0 d} \quad (7.8)$$

where v is the volume of the non-soluble block, a_0 is the surface area of the solvent-phobic block, and d is length of the solvent-phobic block. Amphiphilic ABA

triblock copolymers of hydrophilic poly(2-alkyl-2-oxazoline) end blocks and a central hydrophobic central (B) block of polydimethylsiloxane can form a polymeric vesicle or polymersome or a planar bilayer structure similar to a biological lipid bilayer [12]. A large number of protein channels can be incorporated into these membrane structures providing opportunities for sensor and other applications.

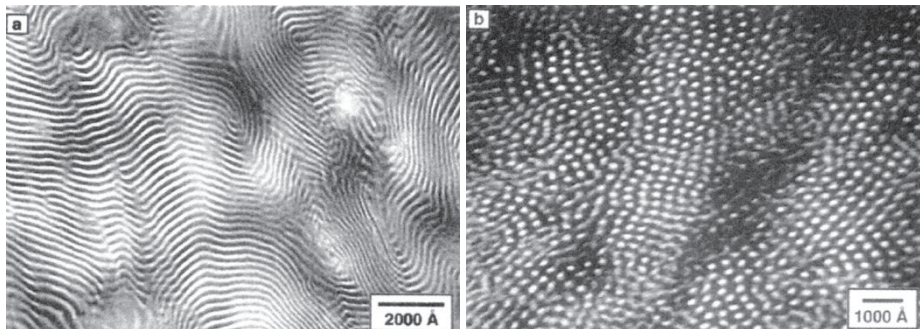


Figure 7-13 TEM micrographs of polyisoprene- β -polystyrene (PI-PS). (a) Lamellar morphology, $f_{\text{PI}} = 0.64$ ($M_n = 3.98 \times 10^4$); (b) hexagonally packed cylinders, $f_{\text{PI}} = 0.82$ ($M_n = 7.01 \times 10^4$). Specimens were annealed at 150°C in vacuum. Reproduced with permission from A. K. Khandpur et al., *Polyisoprene-Polystyrene Diblock Copolymer Phase Diagram near the Order-Disorder Transition*. *Macromolecules*, 1995. **28**: p. 8796–8806. Copyright 1995, American Chemical Society.

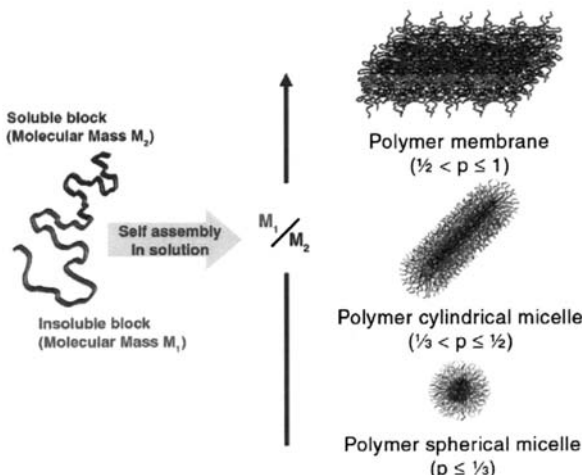


Figure 7-14 Morphological structures formed by amphiphilic triblock copolymers in solvent under different conditions. T. Smart et al., *Block Copolymer Nanostructures*, *Nano Today*, 2008. **3**(3–4): p. 38–46.

7.4 Composites

The first composite materials may have been bricks fashioned by the ancient Egyptians from mud and straw. Commercialization of composites can be traced to early in the twentieth this century when cellulose fibers were used to reinforce phenolic and later urea and melamine resins. Probably the most familiar composite material today is Fiberglas, first introduced in the 1940s. Fiberglas is the trade name for a composite consisting of glass-fiber reinforcement of an unsaturated-polyester matrix. It is widely used to form large lightweight reinforced structures, such as the body of a Corvette, or the hull of a cabin cruiser, or as alternatives to heavy porcelain in the manufacture of bathtubs and shower stalls.

Composites are used in a wide range of applications, wherever high strength-to-weight ratios are important. Principal uses are found in the automotive, marine, and construction industries. In the majority of cases, especially those requiring high performance in the automotive and aerospace industries, the discontinuous phase or filler is in the form of a fiber. Typical fibers for composite applications include carbon or graphite, glass, aromatic polyamide (e.g., Kevlar), and others that were listed in Table 7-2. In some cases, the filler may be particulate—in the form of microspheres or flakes.

In most cases, composite matrices are thermosets, although there has been recent interest in composites made from thermoplastics and composites having carbon, ceramic, or metallic matrices for high-temperature and other demanding applications. The most important class of thermosets for composite use is epoxy (see Section 9.3.1). Although epoxy resins are inexpensive and easy to process, they are brittle and have relatively high moisture absorption, which can affect the strength of the filler–matrix interface. As discussed in the following sections, interfacial strength can be improved by the use of coupling agents, which are low-molecular-weight organic-inorganic compounds that serve to promote adhesion between the filler and matrix. In general, thermoplastics such as polysulfone offer higher impact strength than thermosets but are more susceptible to solvent attack and have higher creep compliance, which results in a loss of dimensional stability under load. Recently, some high-impact semicrystalline thermoplastics, such as polyetheretherketone (PEEK), have been evaluated for composite use due to their good solvent resistance and impact strength. Polyimides, which can be either thermoset or thermoplastic, are widely used in aerospace applications. Thermosetting polyimides provide easier processing and higher heat resistance, while thermoplastic polyimides offer greater toughness. Typical properties of some thermoset and thermoplastic matrices are compared in Table 7-5.

Composites are processed by a variety of methods, including compression and resin-transfer molding, which will be described in Chapter 11. Specialized processing operations for composite fabrication are filament winding and pultrusion,

which will be described in Section 7.4.2. These are used to prepare continuous fiber-reinforced composites with controlled fiber orientation.

Table 7-5 Properties of Composite Matrices

Property	Thermoset Epoxy	Thermoplastics		
	PI ^a	PSF ^b	PEEK ^c	
Compressive strength, MPa	140	187	96	—
Density, g cm ⁻³	1.15–1.2	1.43	1.24	1.32
Modulus, GPa	2.8–4.2	3.2	2.5	3.9
Tensile strength, MPa	55–130	56	70	91
Thermal expansion coefficient, 10^{-6} per °C	45–65	50	—	47
Thermal conductivity, W (m K) ⁻¹	0.17–0.21	0.36	—	0.25
T_g , °C	130–250	370	185	143

^a PI, thermosetting polyimide.

^b PSF, bisphenol-A polysulfone (Udel P1700).

^c PEEK, polyetheretherketone; ca. 35% crystalline with T_m of 334°C.

The mechanical properties of composites are strongly influenced by the size, type, concentration, and dispersion of filler, as well as the extent of interfacial adhesion between the filler and matrix (i.e., continuous phase) and the properties of the matrix. The interrelationships between these variables are complex and only basic principles relating these parameters to the mechanical properties and ultimate performance of particulate and fiber-reinforced composites are developed in the following section.

7.4.1 Mechanical Properties

Modulus. The principal function of reinforcing fillers is to increase the modulus of the composite. This is typically accompanied by an increase in the heat-distortion temperature. The modulus of a glassy-polymer composite containing a rigid *particulate* filler may be estimated by use of the modified *Halpin-Tsai equation* given as

$$\frac{M}{M_m} = \frac{1 + AB\phi_f}{1 - B\psi\phi_f} \quad (7.9)$$

where M is the modulus (tensile, shear, or bulk) of the composite, M_m is the corresponding modulus of the unreinforced matrix polymer, A is a constant that depends on the filler geometry and the Poisson's ratio of the matrix, ϕ_f is the volume fraction of filler, ψ depends upon the maximum *packing* volume fraction of the filler (0.601

for random loose packing of spheres), and B is a function of A and the relative moduli of the filler (M_f) and matrix as

$$B = \frac{(M_f/M_m) - 1}{(M_f/M_m) + A}. \quad (7.10)$$

If the particulate filler is uniformly dispersed, the mechanical properties of a particulate-filled composite are independent of the testing direction (i.e., isotropic). By comparison, the properties of fiber-reinforced composites are dependent upon the direction of measurement—they are *anisotropic*. This is because fibers are usually uniaxially oriented or oriented randomly in a plane during the fabrication of the composite. The maximum modulus of the composite is obtained in the orientation direction. For uniaxially oriented fibers, the tensile (Young's) modulus measured in the orientation direction (the longitudinal modulus, E_L) is given by a simple rule of mixtures as

$$E_L = (1 - \phi_f) E_m + \phi_f E_f \quad (7.11)$$

where E_m is the tensile modulus of the matrix and E_f is the tensile modulus of the fiber (see Table 7-3). The modulus measured in the direction perpendicular to orientation (i.e., the transverse modulus, E_T) is typically much smaller than E_L . It can be expressed in the form of the modified Halpin–Tsai equation (eq. (7.9)) as

$$\frac{E_T}{E_m} = \frac{1 + AB\phi_f}{1 - B\psi\phi_f} \quad (7.12)$$

where A is equal to twice the aspect ratio (L/D) for uniaxially oriented fibers.

Strength. In general, composite strength, an ultimate property, depends upon many factors, such as the adhesive strength of the matrix-filler interphase, and, therefore, is not as easily modeled as is modulus. Interfacial strength may be reduced by the presence of water adsorbed on the filler surface or by thermal stresses resulting from a mismatch between the thermal coefficients of linear expansion for the filler and matrix polymer. Polymers have relatively high linear-expansion coefficients (60 to 80×10^{-6} per °C for PS) compared to fillers such as silica glass (0.6×10^{-6} per °C) or graphite (7.8×10^{-6} per °C).

Several relationships have been proposed to relate the ultimate strength of a *particulate-filled composite* (σ_u) to the ultimate strength of the unfilled matrix (σ_m). One such equation proposed by Schrager [16] is given as

$$\sigma_u = \sigma_m \exp(-r\phi_f) \quad (7.13)$$

where r is an interfacial factor (typically 2.66 for many composites). This provides a maximum value for strength (up to 35 to 40 vol % filler) and assumes good adhe-

sion between the dispersed filler and matrix. Strength of the composite will decrease with decreasing interfacial strength.

In the case of *fiber-reinforced composites*, strength, like modulus, depends on the orientation of the fiber with respect to the stress direction. The maximum strength is obtained for uniaxially oriented fibers when the fibers are oriented in the tensile (or longitudinal) direction, σ_L . In this case, the strength is given by the simple rule of mixtures in the same form as for modulus (eq. (7.11)):

$$\sigma_L = (1 - \phi_f)\sigma_m + \phi_f\sigma_f. \quad (7.14)$$

In contrast, the strength of the uniaxially oriented fiber composite is minimal when the strength is measured transverse to the fiber orientation, σ_T . This strength is strongly influenced by the strength of the interfacial bond and will be much lower than the longitudinal strength. As an approximation, σ_T may be approximated as one-half of the matrix strength, σ_m .

As an illustration of the effect of fiber reinforcement on composite properties, heat-distortion temperature and some mechanical properties of carbon- and glass-fiber composites of polyetheretherketone (PEEK), an engineering thermoplastic (see Section 10.2.3), are given in Table 7-6. As illustrated, reinforcement increases the heat-distortion temperature of PEEK from 148° to 300°C at 30% fiber loading. In addition, tensile strength and especially (flexural) modulus are increased considerably over corresponding values for the unfilled or “neat” resin due to the high modulus and strength of carbon and glass fibers (see Table 7-8). The modulus of the carbon-fiber composite is higher than that of the glass-fiber composite since the modulus of carbon and graphite fibers is greater than that of glass fibers up to a factor of nearly 5.

Table 7-6 Properties of PEEK Composites

Property	PEEK	30% Carbon Fiber	30% Glass Fiber
Flexural modulus (GPa) at 23°C	3.89	15.5	8.0
Heat-deflection temperature °C at 1.82 MPa (264 psi)	148	300	300
Tensile strength (MPa) at 23°C	91.0	146.0	140.0

Interfacial Adhesion and Coupling Agents. In practice, interfacial strength is improved by the use of low-molecular-weight organofunctional silanes (or titanates) such as those listed in Table 7-7, which act as a *coupling agent* bridging the matrix-filler boundary. Typically, these inorganic-organic additives have one or more hydrolyzable groups (e.g., hydroxyl or alkoxy) capable of silanol-group formation for bonding with mineral surfaces and a matrix-specific organofunctional group such as an epoxy functionality, which can react with, or promote adhesion to, the matrix resin. The most important of the coupling agents are the silanes that are

widely used in the form of aqueous dispersions to treat glass fiber and coarse particulate fillers.

Table 7-7 Common Coupling Agents

Type	Representative Structures
Epoxy silane	$\text{H}_2\text{C}=\text{CHCH}_2\text{OCH}_2\text{CH}_2\text{CH}_2\text{CH}_2\text{Si(OCH}_3)_3$
Methacrylate	$\text{H}_2\text{C}=\overset{\text{CH}_3}{\underset{\text{O}}{\text{C}}}(\text{O})-\text{CH}_2\text{CH}_2\text{CH}_2\text{Si(OCH}_3)_3$
Primary amine silane	$\text{H}_2\text{NCH}_2\text{CH}_2\text{CH}_2\text{Si(OC}_2\text{H}_5)_3$
Titanate	$(\text{H}_2\text{C}=\overset{\text{CH}_3}{\underset{\text{O}}{\text{C}}}(\text{O})-\text{C})_3\text{TiOCH}(\text{CH}_3)_2$
Vinyl silane	$\text{CH}_2=\text{CH-Si(OCH}_3)_3$

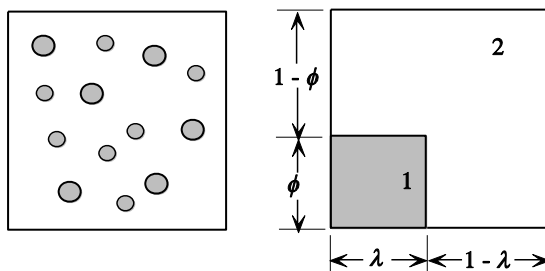
The effect of coupling agents on the dry and wet flexural strength of glass-fiber-reinforced polyester is illustrated in Table 7-8. In this example, a silane-functional coupling agent is shown to greatly improve the flexural strength of the polyester composite, both in the dry state and after immersion in boiling water. Improved interfacial adhesion may also be achieved by modification or functionalization of the fiber surface. For example, the interfacial adhesion of ultrahigh-molecular-weight polyethylene may be improved by plasma treatment in pure oxygen.

Table 7-8 Flexural Strength of a Glass-Reinforced Polyester

Coupling Agent	Flexural Strength (GPa) ^a	
	Dry	2-Hour Boil
None	0.38	0.23
Vinyl silane	0.46	0.41
Methacrylate silane	0.62	0.59

^a To convert GPa to psi, multiply by 145,000.

Dynamic-Mechanical Properties. Dynamic-mechanical measurements (see Section 5.1.1) can be used to investigate the morphology of composites and phase-separated polymer blends through the “equivalent model” originally proposed by Takayanagi [17]. As illustrated in Figure 7-15, the dynamic-mechanical properties of any two-phase morphology, such as an immiscible blend, composite, laminate, or semicrystalline polymer, can be modeled as a series and parallel combination of contributions from the individual components—the matrix and dispersed phases.

**Figure 7-15**

The equivalent model of Takayanagi [17]. An idealized two-phase system consisting of a dispersed phase (shaded regions) dispersed in a matrix of component 1 is shown at the left. This composite structure can be modeled as a unit cube ($1 \times 1 \times 1$) (pictured at right) with the dispersed phase (component 1) having dimensions of $\phi \times \lambda \times 1$ (i.e., the volume fraction is $\phi\lambda$).

The dynamic modulus of the composite can be modeled by resolving the equivalent model pictured at the right of Figure 7-15 as contributions from elements in series and parallel, as illustrated in Figure 7-16. Since elements A and B are in series, strains on these elements, or equivalently their weighted compliances, are additive and, therefore, we can write

$$\frac{D^*}{E^*} = (1 - \phi) D_A^* + \phi D_B^*. \quad (7.15)$$

Since element A is pure component 2 (the matrix component),

$$D_A^* = \frac{1}{E_A^*} = \frac{1}{E_2^*}. \quad (7.16)$$

Element B is a parallel combination of components 1 (dispersed component) and 2 (matrix) and, therefore, stresses or equivalently moduli are additive:

$$\frac{E_B^*}{D_B^*} = \frac{1}{E_1^*} = \lambda E_1^* + (1 - \lambda) E_2^*. \quad (7.17)$$

Substituting eqs. (7.16) and (7.17) into eq. (7.15) gives the final relationship for the dynamic compliance or modulus of the equivalent model as

$$D^* = \frac{1}{E^*} = \frac{1 - \phi}{E_2^*} + \frac{\phi}{\lambda E_1^* + (1 - \lambda) E_2^*}. \quad (7.18)$$

In eq. (7.18), ϕ and λ have the significance of fitting parameters, although the product $(\phi\lambda)$ is equal to the *volume fraction* of the dispersed phase. The values of these fitting parameters obtained by fitting actual dynamic-mechanical data give a quali-

tative understanding of the morphology of the composite. For example, $\lambda = \phi$ indicates a uniformly dispersed phase, while $\lambda < \phi$ indicates agglomeration of dispersed phases.

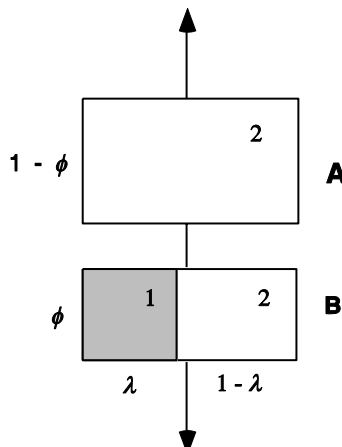


Figure 7-16 Parallel and series elements of equivalent model illustrated in Figure 7-15. Elements A and B are in series combination to the applied strain (arrows). Element B is composed of two elements (dispersed phase and matrix) in parallel.

7.4.2 Composite Fabrication

As previously indicated, composites can be fabricated by a variety of techniques, including compression and resin-transfer molding, which are discussed in Chapter 11. Composites used for nonstructural (i.e., non-load-bearing) applications are produced by using sheet-molding compound (SMC), bulk-molding compound (BMC), preform molding, injection molding, and spray-up. For the manufacture of composites for structural applications, two important processing methods are filament winding and pultrusion, which are reviewed here.

In general, BMC consists of styrenated unsaturated-polyester resin (unsaturated polyester containing styrene monomer, which is polymerized during the final cure process), a low-profile thermoplastic polymer, an inert filler such as calcium carbonate, glass fibers, a polymerization initiator, and other additives such as a lubricant (e.g., zinc stearate), and a maturation agent (e.g., MgO). BMC has the consistency of putty, which can be applied with a trowel. A related composite formulation is SMC, which is formed by combining styrenated polyester resin thickened by 1% of calcium or magnesium oxide, fillers, peroxides, and chopped glass fibers. The SMC is contained between layers of polyethylene film, which are removed at

the time of molding. In spray-up, glass fibers and a resin are simultaneously deposited in a mold. In this process, a roving (8 to 120 strands of glass fiber) is fed through a chopper and ejected into a resin stream. A preform refers to a preshaped composite formed by distribution of chopped fibers by air, water flotation, or vacuum over the surface of a preformed screen. A preform may also refer to a mat or cloth preformed to a specific shape on a mandrel or mock-up.

Filament Winding. A simple filament-winding operation is illustrated in Figure 7-17. Fibers are pulled from bobbins through a bath containing the composite resin, such as an epoxy or (unsaturated) polyester formulation, and then the impregnated fibers are wound onto a form (the mandrel) in some predetermined arrangement. Usually, fibers are E- or S-glass (see Table 7-3). Once the mandrel is uniformly covered to the desired thickness and fiber orientation, the composite is cured at an elevated temperature and the mandrel may be removed or left as an integral part of the composite. Filament winding may be used to prepare corrosion-resistant (fiber-glass) tanks and pipes. Employing advanced resin materials, filament winding is also being used to prepare high-performance composites for structural and other applications in the automotive and aerospace industries. The continuous reinforcement and controlled fiber orientation that can be achieved by filament winding provide a higher level of reinforcement than is possible by discontinuous reinforcement using individual fibers.

Pultrusion. A simplified diagram of a pultrusion operation is illustrated in Figure 7-18. Compared to filament winding, pultrusion is a completely continuous process operation since the cure step is online. This makes pultrusion a suitable process for commercial production lines producing of a variety of composite shapes or profiles. A roving* of continuous fibers (e.g., E-glass) and a continuous-strand mat (typically glass/polyester) are combined and immersed in a resin bath before passing through a forming guide and the curing oven. The majority of composites that are pultruded are the fiber-glass variety prepared from unsaturated polyester resin and E-glass. Fiber loadings in pultrusion may range from 20% to 80%.

* When graphite or boron fibers are used in place of glass fibers, the term *tow* is used rather than *roving*.

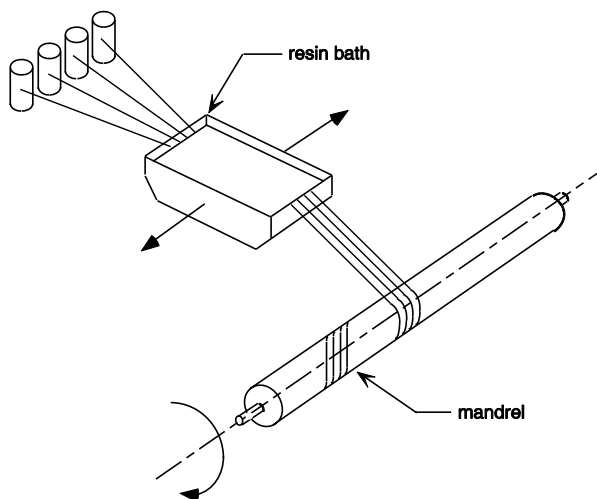


Figure 7-17 Filament-winding operation. Adapted from R. C. Hayes in *The Concise Encyclopedia of Polymer Science and Engineering*, J. I. Kroschwitz, ed. Copyright © 1990 by John Wiley & Sons. This material is used by permission of John Wiley & Sons, Inc.

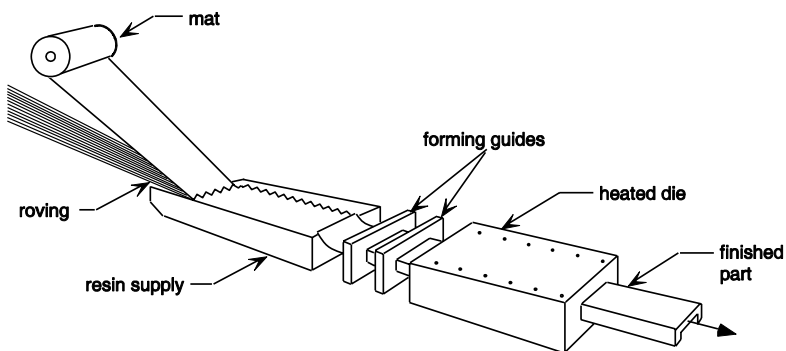


Figure 7-18 Pultrusion line. Adapted from D. Evans in *The Concise Encyclopedia of Polymer Science and Engineering*, J. I. Kroschwitz, ed. Copyright © 1990 by John Wiley & Sons. This material is used by permission of John Wiley & Sons, Inc.

7.5 Nanocomposites

One of the most rapidly growing areas of polymer technology is that of nanocomposites. Compared to more traditional composite materials described in the previous

section, the distinguishing characteristic of nanocomposites is the size of the reinforcing filler. In nanocomposites, this reinforcing filler (the nanofiller) is typically a carbon- or silicon-based high-aspect-ratio (10:1 to 1000:1) reinforcement that has one or more dimensions in the range from 1 to 100 nm (10 to 1000 Å). As covered in greater detail in Section 7.5.1, nanofillers include organically modified clay (montmorillonite or MMT), organically modified silicon–oxygen nanocages (POSS*), single- and multi-walled carbon nanotubes (CNTs), carbon nanofiber (CNF), graphene (single-sheet graphite), nanosilica (e.g., Aerosil), various metal oxides such as indium tin oxide (ITO), and graphite nanoparticles. Some of the attractive properties of nanocomposites include improved electrical and mechanical properties (e.g., increased strength and modulus without sacrificing impact properties), reduced gas and water permeability for barrier applications (e.g., packaging and fuel containment), increased thermal stability, flame resistance, and resistance to wear, elevated heat-distortion temperature, recyclability, potential for surface and interface modification, enhanced ionic conductivity, and improved processability (e.g., extrusion and molding). Other advantages include increased dimensional stability at elevated temperatures, better surface gloss, increased tear resistance of elastomers, optical transparency, accelerated cure of elastomers, and reduced shrinkage. Perhaps the earliest commercial nanocomposites were fabricated in the 1980s from nylon-6 and MMT by researchers at Toyota. Since the early work by Toyota, the market for nanocomposites has increased rapidly and is expected to reach 11 billion pounds by 2020 in the United States alone. In addition to nylon-6, nanocomposites have been prepared from many commodity and engineering-grade thermoplastics including nylon-11, polysiloxanes, poly(ethylene oxide), polyetherimide, some thermoplastic elastomers, and a variety of thermosets including epoxies, phenolic resins, and cyanate ester. Covered in the following section are MMT and the properties of nanocomposites of MMT. Section 7.5.2 provides coverage of other important nanofillers and their corresponding nanocomposites.

7.5.1 Montmorillonite Nanocomposites

Montmorillonite. The most common form of nano-reinforcement has been organoclay derived from montmorillonite (MMT). MMT is a naturally occurring 2:1 phyllosilicate with the same structure as talc and mica, but a different layer charge. Modification of the inorganic surface of MMT by organic treatment is used to increase dispersion in the polymer matrix. The crystal structure of MMT consists of 1-nm thin layers with a central octahedral sheet of alumina fused between two external silica tetrahedral sheets. These platelets have thicknesses of ~1 nm with as-

* Polyhedral oligomeric silsesquioxane or POSS, a trademark of Hybrid Plastics.

pect ratios (i.e., diameter:thickness) from 10:1 to 1000:1 and are arranged in stacks that can be separated (or exfoliated) during composite fabrication. Isomorphous substitution within the layers (e.g., replacing Al^{3+} by Mg^{2+}) can be used to modify the charge-exchange capacity. The silicate sheets in MMT are separated by cations, typically sodium, as illustrated in Figure 7-19. These cations balance the overall charge. The sodium cation in the gallery can be exchanged with other cations such as lithium, potassium, and calcium. In water, large organic cations, such as an alkyl ammonium cation, can replace the sodium cation in the swollen layered silicates. Some specific examples include dimethyl distearyl ammonium chloride and dimethyl stearyl benzyl ammonium chloride. The choice of the alkyl group can be tailored to improve miscibility of MMT with a specific polymer matrix. For example, silicone rubber nanocomposites can be fabricated by ion-exchanging Na^+ /MMT with dimethyl ditallow ammonium bromide or hexadecyltrimethylammonium bromide. The ion-exchange process also increases the gallery height in relation to the molecular size of the organic cation.

For use in nanocomposites, the layered silicates of MMT are generally rendered organophilic by exchanging the Na^+ in a water-swollen layered silicate with an organic cation such as an alkyl ammonium ion. This ion-exchange process increases the gallery height in relation to the molecular size of the organic cation. The choice of an ammonium ion is influenced by its chemical compatibility with the composite matrix. Some examples include dimethyl distearyl ammonium chloride and dimethyl stearyl benzyl ammonium chloride. Organo-MMT nanocomposites of silicone rubber can be fabricated by ion-exchanging Na^+ /MMT with dimethyl ditallow ammonium bromide or hexadecyltrimethylammonium bromide.

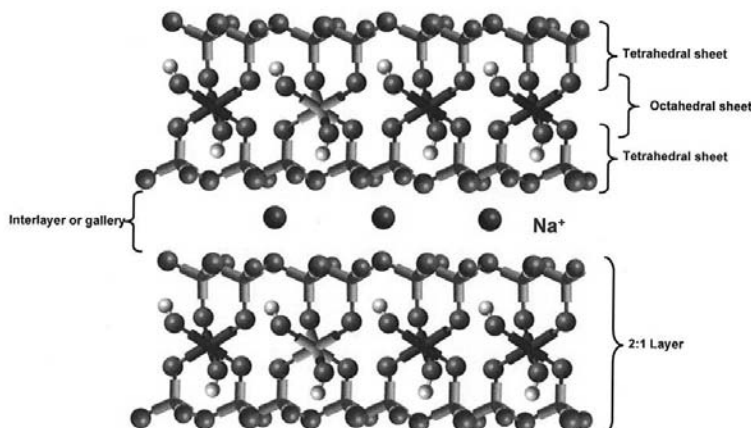


Figure 7-19 Structure of sodium montmorillonite. Courtesy of Southern Clay Product, Incorporated.

Processing. Various ways that polymer chains can be incorporated in organophilic layered silicates during melt processing are illustrated in Figure 7-20. Other than simply mixing the layered silicate with the polymer chains to form a microcomposite, individual polymer chains can be intercalated into each silicate layer. This causes an increase in the interlayer distance over that of the ion-exchanged silicate alone. Alternatively, individual silicate layers can be separated (exfoliated). A nanocomposite also can be prepared by mixing the ion-exchanged layered silicate with a monomer followed by polymerization.

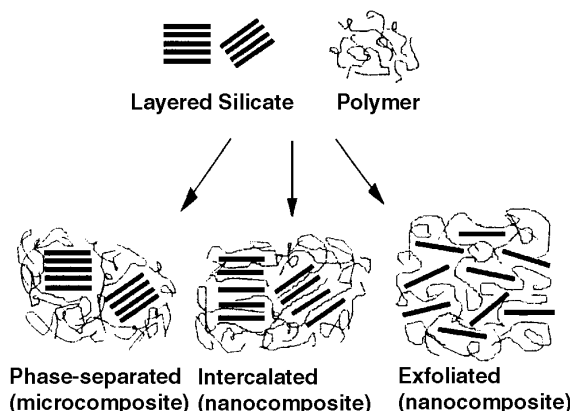


Figure 7-20 Three routes to polymer–silicate structures. From Günter Beyer, *Nanocomposites: a New Class of Flame Retardants for Polymers*, Polymer News, 2001, 25: p. 370. Copyright 2001. Reproduced with permission of Taylor & Francis, Inc., <http://www.routledge-ny.com>.

Properties. One of the unique advantages of nanocomposites, in general, is that property improvement can be significant at much smaller loading than for typical composites made with larger reinforcements such as glass and carbon fibers. This is clearly illustrated for nylon-6 in Figure 7-21 where the relative Young's modulus (ratio of composite modulus to matrix modulus) of a glass-fiber composite is compared to that of an MMT nanocomposite. As shown, the modulus of nylon-6 doubles at 8 wt% MMT compared to 20 wt% glass fiber that is required for the same reinforcement. Other properties of a nylon/MMT nanocomposite are given in Table 7-9. In addition to significant modulus increase, the heat-distortion temperature (HDT) is significantly increased as would be expected due to the reinforcement. While water absorption and impact strength are not significantly affected by MMT reinforcement, the coefficient of thermal expansion is significantly *reduced* while tensile strength is increased. In other studies, significant increases in HDT, modulus, and strength have been reported for MMT nanocomposites of bisphenol-A polysulfone at 3 wt% loading with little loss in elongation at break or impact strength [18]. At higher loading, exfoliation decreases and mechanical properties

decline. A modulus increase of about 50% has been reported for a polyimide/MMT nanocomposite [19] and about 100% for polydimethylsiloxane with only 1% MMT loading.

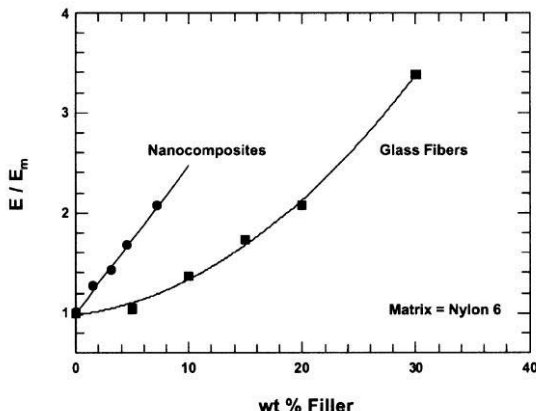


Figure 7-21 Comparison of relative modulus at different concentrations of glass fiber and MMT in nylon-6. Reproduced with permission from T. D. Forres and D. R. Paul, *Modeling Properties of Nylon 6/Clay Nanocomposite Using Composite Theories*. Polymer, 2003. **4**: p. 4993–5013.

Table 7-9 Representative Properties of a Nylon-6 Nanocomposite

Property	Nylon-6	Nanocomposite
Coefficient of thermal expansion ($\times 10^5$)	13	6.3
Heat-distortion temperature (°C)	65	145
Tensile modulus (GPa)	1.1	2.1
Tensile strength (MPa)	69	107
Impact strength (kJ m^{-2})	2.3	2.8
Water absorption (%)	0.87	0.51

7.5.2 Buckyballs, Carbon Nanotubes, Graphene, and POSS

In addition to MMT, nanocomposites can be formed from a wide variety of nano-fillers including those with a carbon base, principally fullerenes, nanotubes, and graphene. Another common nanofiller has the structure of a silicon–oxygen nanocage that can be functionalized with a wide variety of substituent groups including halogens and a number of organic groups such as methyl, ethyl, ethylene, and phenyl.

Buckyballs. The development of nanotechnology was greatly accelerated by the 1985 discovery of the formation of 60 carbon atom clusters when graphite was

vaporized by laser irradiation. This discovery was reported [20] by Richard Smalley and co-discoverers Robert Curl and Harold Kroto.* This work was an outcome of a study to investigate how long-chain carbon molecules may be formed in interstellar space. Smalley speculated that the resulting structure, subsequently termed a *buckyball* or buckminsterfullerene (C_{60}) was a polygon containing 60 vertices and 32 faces, of which 12 were pentagonal and 20 were hexagonal as illustrated by the soccer ball shown in Figure 7-22A and the simulation model in Figure 7-22B.

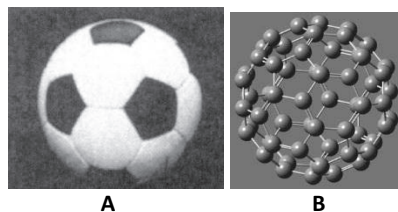


Figure 7-22 **A.** Type of soccer ball used by Smalley to illustrate his 1985 model. **B.** A computer-generated ball-and-stick representation of a buckyball.

Carbon Nanotubes. Carbon nanotubes (CNTs) are the hollow-fiber equivalent of the buckyball. The first single-walled carbon nanotube (SWNT) was produced in 1991 by Sumio Iijima [21] working at NEC in Japan. After the isolation of SWNTs was announced in 1993, Smalley found that by impregnating iron, cobalt, or nickel catalysts in graphite rods that had been used to prepare buckyballs using laser vaporization, an SWNT could be produced. Between 1993 and his untimely death in 2005, Smalley continued to improve the technology of making better CNTs, including producing them in solution and chemical-reacting them to attach functional groups. In general, CNTs provide an attractive combinations of high flexibility and strength combined with high stiffness and low density. SWNTs have diameters approximately 0.4 to 3 nm in diameter and exhibit good electrical properties but are relatively expensive to make.

The typical tensile strength of a CNT is in the range from 100 to 600 GPa or about two orders of magnitude greater than a typical carbon fiber (CF). Densities are approximately 1.3 g cm^{-3} compared to 1.8 to 1.9 g cm^{-3} for CF. Young's modulus is 1–5 TP, compared to 750 GPa for CF. CNTs can carry large current densities with thermal conductivities around 200 W/(mK) . For favorable interactions with a polymeric matrix, CNTs are chemically modified and require good dispersion that can be achieved through in situ polymerization of the matrix, shear mixing, the use of surfactants, and solution processing.

* For their work, Smalley, Curl, and Kroto shared the 1996 Nobel Prize in chemistry.

In addition to SWNTs, multi-walled CNTs (MWNTs) can be prepared. A comparison of computer-generated simulations of an SWNT and a double-walled CNT is shown in Figure 7-23. The projected 2014 market for CNTs given in Table 7-10 is roughly comparable for SWNTs and MWNTs with principal applications in electronics and automotive industries. At present, MWNTs are easier to produce on large scale than are SWNTs and are, therefore, less expensive. Outer diameters of MWNTs are in the range from 2 to 25 nm, significantly larger than SWNTs, with lengths in the range between 0.2 and 2 mm. A typical modulus of MWNTs is 1.8 TPa compared to 0.517 TPa for graphite. They are less brittle than graphite and have a tensile strength of 63 GPa (compared to 1.2 GPa for steel).

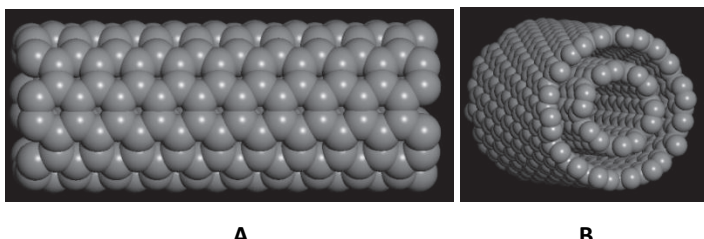


Figure 7-23 Computer simulations of (A) CPK representation of a single-wall CNT (side view); (B) CPK representation of a double-wall CNT (end view).

**Table 7-10 Projected 2014 Market
for Carbon Nanotubes (Total: \$1.07
Billion)**

Total Demand	\$Billion
Type	
SWNT	600
MWNT	479
End Use	
Electronic	394
Automotive	165
Aerospace/defense	65
Other	445

Graphene. A recent addition to a growing list of important nanofillers is graphene. Graphene is a two-dimensional, one-atom-thick allotrope of sp^2 bonded carbon atoms packed in a honeycomb structure. Graphene samples of two to four layers in thickness can be prepared by an arc-discharge procedure. Graphene has many unusual properties including high electron transport (higher conductivity and thermal conductivity than copper but 25% of the weight), superior thermal conductivity, great mechanical strength, and remarkable flexibility and is an absolute barrier material. As shown in Figure 7-24, the tensile strength of an epoxy nanocomposite

containing 1 wt% graphene platelets (GPL) content exceeds that of the same epoxy nanocomposite containing 1 wt% SWNT or 1 wt% MWNT.

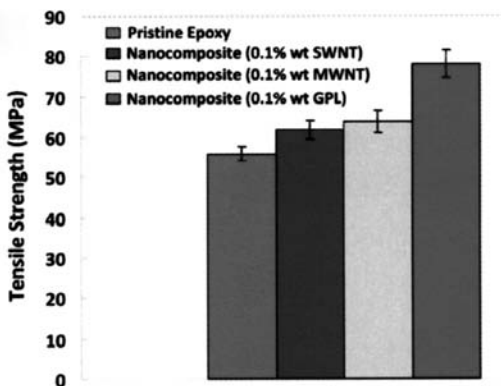


Figure 7-24 Uniaxial tensile testing of epoxy and epoxy nanocomposite with 0.1% of different nanofillers. Reproduced from M. A. Rafiee et al., *Enhanced Mechanical Properties of Nanocomposites at Low Graphene Content*. ACS Nano, 2009. 3(12): p. 3884–3890.

The ultrahigh electron mobility of graphene and its room-temperature quantum Hall effect open unique opportunities for applications in electronics, particularly as a potential competitor to silicon-based devices. Potential applications include high-performance electronics, sensors, computer chips, and energy storage. Graphene was first produced by the mechanical exfoliation of graphite. Other approaches include liquid-phase exfoliation, unzipping carbon nanotubes, chemical vapor deposition, the epitaxial growth on electrically insulating substrates, mechanical exfoliation of graphene from bulk graphite, and the reduction of graphene derivatives (e.g., graphene oxide). A major technological challenge is the controlled production of large sheets. For their work with graphene, Andre Geim and Konstantin Novoselov shared the 2010 Nobel Prize in physics.

POSS. Polyhedral oligomeric silsesquioxane (POSS) can serve both as a multi-functional additive providing molecular-level reinforcement as well as a processing aid and flame retardant [22]. POSS is a cubic form of silica with dimensions in the range of 1 to 3 nm and eight organic groups at its vertices. A (T8) nanocage having all hydrogen substituents is shown in Figure 7-25. Larger nanocages having 10 (T10) and 12 (T12) Si atoms are available. T8 POSS has the formula $(\text{SiO}_{1.5})_8\text{R}_8$ where R represents a halogen atom or an organic group such as alkyl, aryl, cycloaliphatic, vinyl, nitrile, alcohol, isocyanate, glycidyl, or vinyl. A vinyl group can serve to copolymerize with other monomers or oligomers while other groups may serve to promote compatibility with the matrix. POSS nanocomposites exhibit elevated T_g

and decomposition temperature, increased thermal stability, higher modulus and melt strength, improved resistance to oxidation, and reduced flammability due to a significant reduction of the heat-release rate. Other advantages include increased service temperature, low density, low thermal conductivity, thermo-oxidative resistance, and aging resistance. Polymeric materials that have been used for POSS nanocomposites include epoxies, phenolic resins, polysiloxanes, polyimides, poly(propylene oxide), polycarbonate, polyethylene, polyurethanes, ethylene-propylene copolymers, poly(3-hydroxy alkenoates), and polypropylene.

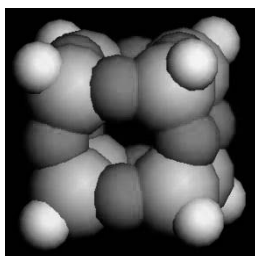


Figure 7-25 Computer representation (CPK model) of octahydrosilsesquioxane ($H_8Si_6O_{12}$). The hydrogen atoms can be replaced by a number of different groups to improve compatibility of the POSS filler with the polymer matrix.

SUGGESTED READING

BLENDS

- Bucknall, C. B., *Toughened Plastics*. 1977, London: Applied Science Publishers Ltd.
- Olabisi, O., *Interpretations of Polymer-Polymer Miscibility*. Journal of Chemical Education, 1981. **68**: p. 944.
- Olabisi, O., L. M. Robeson, and M. T. Shaw, *Polymer-Polymer Miscibility*. 1979, New York: Academic Press.
- Paul, D. R., and S. Newman, *Polymer Blends*. 1978, New York: Academic Press.
- Takayanagi, M., H. Harima, and Y. Iwata, *Viscoelastic Behavior of Polymer Blends and Its Comparison with Model Experiments*. 1963, Memoirs of the Faculty of Engineering Kyushu University, p. 1.
- Weber, M., *Polymer Blends: Materials with Versatile Properties*. Macromolecular Symposium, 2001. **163**: p. 235–250.

INTERPENETRATING NETWORKS

- Barrett, L. W., and L. H. Sperling, *Today's Interpenetrating Polymer Networks*. Trends in Polymer Science, 1993. **1**(2): p. 45.

Sperling, L. H., *Interpenetrating Polymer Networks and Related Materials*. 1981, New York: Plenum Press.

Sperling, L. H., *Interpenetrating Polymer Networks: An Overview*, in *Interpenetrating Polymer Networks*, D. Klempner, L. H. Sperling, and L. A. Utracki, eds., Advances in Chemistry Series. 1984, Washington, DC: American Chemical Society. **239**: p. 3–38.

BLOCK COPOLYMERS

Darling, S. B., *Directing the Self-Assembly of Block Copolymers*. Progress in Polymer Science, 1996. **32**: p. 1152.

Malinova, V., S. Belegrinou, D. de Bruyen Ouboter, and W. Meier, *Biomimetic Block Copolymer Membranes*. Advances in Polymer Science, 2010. **224**: p. 113.

COMPOSITES

Delmonte, J., *Technology of Carbon and Graphite Fiber Composites*. 1981, New York: Van Nostrand Reinhold.

Diefendorf, R. J., and E. Tokarsky, *High-Performance Carbon Fibers*. 1975, Polymer Engineering and Science. 1975, **15**: p. 150.

Lubin, G., ed., *Handbook of Composites*. 1982, New York: Van Nostrand Reinhold.

Nicolais, L., *Mechanics of Composites*. Polymer Engineering and Science, 1975. **15**: p. 137.

Nielsen, L. E., *Mechanical Properties of Polymers and Composites*. 1977, New York: Marcel Dekker, Inc.

Tsai, S. W., and H. T. Hahn, *Introduction to Composite Materials*. 1980, Westport: Technomic Publishing Company.

NANOCOMPOSITES

Brune, D. A., and J. Bicerano, *Micromechanics of Nanocomposites: Comparison of Tensile and Compressive Elastic Moduli, and Prediction of Effects of Incomplete Exfoliation and Imperfect Alignment on Modulus*. Polymer, 2002. **43**: p. 369.

Krishnamoorti, R., and R. Vaia, eds., *Polymer Composites: Synthesis, Characterization, and Modeling*. 2002, Washington, DC: American Chemical Society.

Paul, D. R., and L. M. Robeson, *Polymer Nanotechnology: Nanocomposites*. Polymer, 2008. **49**: p. 3187.

Slia, D., C. T. Hui, S. D. Burnside, and E. P. Giannelis, *An Interface Model for the Prediction of Young's Modulus of Layered Silicate-Elastomer Nanocomposites*. Polymer Composites, 1998. **19**: p. 608.

Vaia, R. A., and E. P. Giannelis, *Polymer Nanocomposites: Status and Opportunities*, MRS Bulletin, May 2001, p. 394.

PROBLEMS

7.1 Poly(2,6-dimethyl-1,4-phenylene oxide) (PPO) is blended with polystyrene. Compare the predictions of the inverse rule of mixtures and the logarithmic rule of mixtures (see Section 4.3.4) by plotting the calculated T_g of the blend against the weight fraction of PS. T_g values obtained from DSC measurements are as follows:

Wt% PPO	T_g (°C)
0	105
20	121
40	140
60	158
80	185
100	216

7.2 For a graphite-fiber composite of polysulfone containing 40 vol % filler, what are the maximum modulus and maximum strength that can be expected?

7.3. Draw the chemical structures for the following plasticizers:

- (a) TCP
- (b) TOTM
- (c) DOA
- (d) DIOP

7.4 Give your best estimate for the T_g of PVC plasticized with 30 phr of TOTM ($T_g = -72^\circ\text{C}$).

7.5 Explain why the curve representing the T_g of miscible TMPC/PS blends appearing in Figure 7-4 appears to diverge at low TMPC compositions.

7.6 Show that the Halpin–Tsai equation (eq. (7.9)) reduces to the simple law of mixtures

$$M = \phi_1 M_1 + \phi_2 M_2$$

when the Halpin–Tsai parameter A approaches infinity and reduces to the inverse rule of mixtures

$$\frac{1}{M} = \frac{\phi_1}{M_1} + \frac{\phi_2}{M_2}$$

when A approaches zero.

7.7 Inverse gas chromatography (see Section 3.2.5) can be used to determine an apparent Flory interaction, $\chi'_{23,\text{app}}$, using a solvent probe through the relationship [23]

$$\chi'_{23,\text{app}} = \ln\left(\frac{V_{g,\text{blend}}}{w_2 v_2 + w_3 v_3}\right) - \phi_2 \ln\left(\frac{V_{g,2}}{v_2}\right) - \phi_3 \ln\left(\frac{V_{g,3}}{v_3}\right)$$

where w and v are weight fraction and specific volume, respectively. Specific retention volumes for polystyrene (2), poly(2,6-dimethyl-1,4-phenylene oxide) (PPO) (3), and a 50/50 blend of PPO and polystyrene using toluene as the probe at 270°C are given below. From these data, calculate χ'_{23} for the PPO/PS blend. Is this value consistent with the reported miscibility of this blend?

Coating	V_g (mL/g-coating)
PS	2.38
PPO	2.96
PPO/PS	2.42

7.8 Discuss the current market and methods of producing single-walled and multi-walled carbon nanotubes.

REFERENCES

1. Kelley, F. N., and F. Bueche, *Viscosity and Glass Temperature Relations for Polymer–Diluent Systems*. Journal of Polymer Science, 1961. **50**: p. 549–556.
2. Wood, L. A., *Glass Transition Temperatures of Copolymers*. Journal of Polymer Science, 1958. **28**: p. 319–330.
3. Gordon, M., and S. J. Taylor, *Ideal Copolymers and the Second-Order Transitions of Synthetic Rubbers. I. Non-Crystalline Copolymers*. Journal of Applied Chemistry, 1952. **2**: p. 493–500.
4. Penzel, E., J. Rieger, and H. A. Schneider, *The Glass Transition Temperature of Random Copolymers. I. Experimental Data and the Gordon-Taylor Equation*. Polymer, 1997. **38**(2): p. 325–337.
5. Fried, J. R., G. A. Hanna, and H. Kalkanoglu, *Compatibility Studies of PPO Blends*, in *Polymer Compatibility and Incompatibility—Principles and Practice*, K. Solc, ed. 1982, New York: Harwood Academic Publishers, p. 237–248.
6. Illers, K.-H., W. Heckmann, and J. Hambrecht, *Untersuchung des Mischungsgleichgewichts binärer Polymermischungen. I. Mischungen aus Polystyrol und Tetarmethyl-bisphenol A-Polycarbonat*. Colloid and Polymer Science, 1982. **262**: p. 557–565.
7. Scott, R. L., *The Thermodynamics of High Polymer Solutions. V. Phase Equilibria in the Ternary System: Polymer 1-Polymer 2-Solvent*. Journal of Chemical Physics, 1949. **17**: p. 279–284.
8. McMaster, L. P., *Aspects of Polymer-Polymer Thermodynamics*. Macromolecules, 1973. **6**: p. 760–773.

9. Goh, S. H., and K. S. Siow, *Calorimetric Study of the Miscibility of Poly(Styrene-co-Acrylonitrile)/Poly(Methyl Methacrylate)/Poly(Ethyl Methacrylate) Ternary Blends*. *Thermochimica Acta*, 1986. **105**: p. 191–195.
10. Paul, D. R., and J. O. Altamirano, in *Copolymers, Polyblends, and Composites*, N. A. J. Platzer, ed., 1975, Washington DC: American Chemical Society. p. 371–385.
11. Cieslinski, R. C., *Real-Time Deformation of Polymers in the Transmission Electron Microscope*. *Journal of Materials Science Letters*, 1992. **11**: p. 813–816.
12. Kita-Tokarczyk, K., et al., *Block Copolymer Vesicles—Using Concepts from Polymer Chemistry to Mimic Biomembranes*. *Polymer*, 2005. **46**: p. 3540–3563.
13. Matsen, M. W., and F. S. Bates, *Unifying Weak- and Strong-Segregation Block Copolymer Theories*. *Macromolecules*, 1996. **29**(4): p. 1091–1098.
14. Bates, F. S., and G. H. Fredrickson, *Block Copolymers—Designer Soft Materials*. *Physics Today*, February 1999. p. 32–38.
15. Smart, T., et al., *Block Copolymer Nanostructures*. *Nanotoday*, 2008. **3**(3–4): p. 38–46.
16. Schrager, M., *The Effect of Spherical Inclusions on the Ultimate Strength of Polymer Composites*. *Journal of Applied Polymer Science*, 1978. **22**: p. 2379–2381.
17. Takayanagi, M., H. Harima, and Y. Iwata, *Viscoelastic Behavior of Polymer Blends and Its Comparison with Model Experiments*. *Memoirs of the Faculty of Engineering, Kyushu University*, 1963. **23**: p. 113.
18. Sur, G. S., et al., *Synthesis, Structure, Mechanical Properties, and Thermal Stability of Some Polysulfone/Organoclay Nanocomposites*. *Polymer*, 2001. **42**: p. 9783–9789.
19. Tyan, H.-L., K.-H. Wei, and T.-E. Hsieh, *Mechanical Properties of Clay-Polyimide (BTDA-ODA) Nanocomposite via ODA-Modified Organoclay*. *Journal of Polymer Science: Part B: Polymer Physics*, 2000. **38**: p. 2873–2878.
20. Kroto, H. W., et al., *C_{60} : Buckminsterfullerene*. *Nature*, 1985. **318**: p. 162–163.
21. Iijima, S., *Helical Microtubules of Graphitic Carbon*. *Nature*, 1991. **354**: p. 56–58.
22. Koo, J. H., and L. A. Pilato, *Polymer Nanostructured Materials for High Temperature Applications*. *SAMPE Journal*, 2005. **41**(2): p. 7–19.
23. Al-Saigh, Z. Y., and P. Munk, *Study of Polymer-Polymer Interaction Coefficients in Polymer Blends Using Inverse Gas Chromatography*. *Macromolecules*, 1984: p. 803–809.